Technical Report

Description and Features of UX-Analyze

ESTCP Project MM-0210

February 2009

Dean Keiswetter
SAIC

Environmental Security Technology
Certification Program

Report Documentation Page

Form Approved
OMB No. 0704-0188

1. REPORT DATE	2. REPORT TYPE	3. DATES COVERED
FEB 2009		**00-00-2009 to 00-00-2009**

4. TITLE AND SUBTITLE	5a. CONTRACT NUMBER
Description and Features of UX-Analyze	5b. GRANT NUMBER
	5c. PROGRAM ELEMENT NUMBER
6. AUTHOR(S)	5d. PROJECT NUMBER
	5e. TASK NUMBER
	5f. WORK UNIT NUMBER
7. PERFORMING ORGANIZATION NAME(S) AND ADDRESS(ES) **Science Applications International Corporation (SAIC),1710 SAIC Drive ,McLean,VA,22102**	8. PERFORMING ORGANIZATION REPORT NUMBER
9. SPONSORING/MONITORING AGENCY NAME(S) AND ADDRESS(ES)	10. SPONSOR/MONITOR'S ACRONYM(S)
	11. SPONSOR/MONITOR'S REPORT NUMBER(S)

12. DISTRIBUTION/AVAILABILITY STATEMENT
Approved for public release; distribution unlimited

13. SUPPLEMENTARY NOTES

14. ABSTRACT

15. SUBJECT TERMS

16. SECURITY CLASSIFICATION OF:			17. LIMITATION OF ABSTRACT	18. NUMBER OF PAGES	19a. NAME OF RESPONSIBLE PERSON
a. REPORT	b. ABSTRACT	c. THIS PAGE			
unclassified	**unclassified**	**unclassified**	**Same as Report (SAR)**	**42**	

Contents

Figures

Acknowledgements

This work was funded by the Environmental Security Technology Certification Program Office, under MM-0210, entitled 'Feature-based UXO Detection and Discrimination'. It was performed by a team of personnel from Science Applications International Corporation (SAIC), Duke University, and Geosoft Incorporated.

We gratefully acknowledge Dr. Anne Andrews, Program Manager of ESTCP's Munitions Management Thrust Area, and Dr. Jeff Marqusee, ESTCP Director, for their vision, support, and guidance throughout the life of this project.

The Principal Investigators for this project are Dr. Dean Keiswetter, SAIC, and Dr. Leslie Collins, Duke University. Key technical contributors include Mr. Tom Furuya, SAIC, Dr. Tom Bell, SAIC, Ms. Chunmei Yang, Duke University, and Ms. Elizabeth Baranyi, Geosoft Incorporated.

Summary

UX-Analyze is an analysis framework within Oasis montaj™ that integrates quantitative analysis algorithms and custom-designed visualization schemes. UX-Analyze was conceived, coded, and validated in partial fulfillment of MM-0210. Transparency is achieved by leveraging the professional, flexible, and visual computing environment inherent in Oasis montaj™. The analysis algorithms provide quantitative evaluation criteria (e.g., target characterization and classification) by assuming a dipolar source and deriving the best set of induced dipole model parameters that account for the spatial variation of the signal. The model parameters are target location and depth, three principal axis polarizations corresponding to the principle axes of the target (EMI only), and the three angles that describe the orientation of the target. The source's size can be estimated using empirical relationships between either the dipole moment for magnetic data or the sum of the targets' response coefficients. After evaluating multiple classifiers we embedded the generalized likelihood ratio test into UX-Analyze. Data from single sensors or from fixed-geometry arrays of sensors can also be inverted using UX-Analyze.

1. Overview

UX-Analyze combines physics-inspired characterization and classification routines with Geosoft's' commercial data processing product, Oasis montaj. It is a target selection, fitting and classification tool for UXO applications. UX-Analyze provides geophysicists with an easy-to-use and comprehensive UXO classification tool for both magnetic and electromagnetic data. UX-Analyze allows users to systematically identify, extract, edit, and store data around individual anomalies. It provides efficient data structures and access for the analysis algorithms, stores the fitted parameters, and allows for multiple data types and surveys. This module is the interface between Oasis montaj and phenomenological inversion software (Figure 1-1).

We chose to embed our analysis routines in the Oasis montaj software suite because Geosoft's Oasis montaj is a powerful processing and mapping software used by many in the UXO services sector. It also is used for mineral exploration, oil and gas exploration, and earth sciences investigations. The software package includes a rich set of built-in data import, processing, visualization, mapping, and integration capabilities. To minimize the learning curve and maximize user acceptance, we adopted the look and feel of Oasis montaj.

This document summarizes the logic, features, and operations of UX-Analyze. Additional information regarding operating details, including sample data sets and analysis steps, can be found via the online help menu that accompanies Oasis montaj.

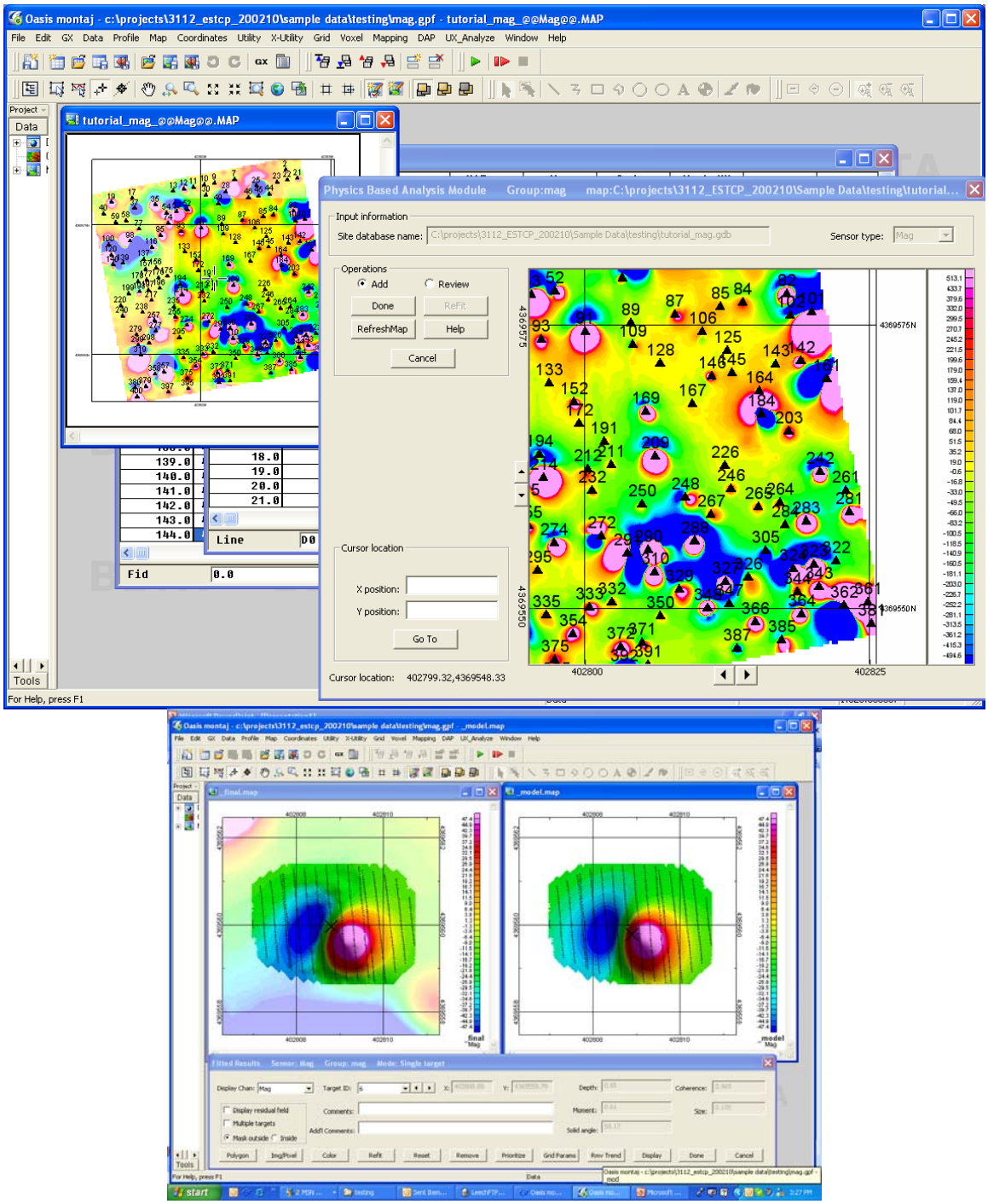

Figure 1-1 Screen snapshots of the computer monitor during data analysis using UX-Analyze. The graphical user interface (GUI) for searching, identifying, and reviewing anomalies is shown on top while the modeling GUI is shown below.

2. Features

2.1 Look and Feel

UX-Analyze provides tools to view magnetic or electromagnetic data collected over a large survey area and select targets via a number of different methods. The anomaly selections can be performed outside of the UX-Analyze suite and imported, or alternatively, manually identified via an interactive module. The look and feel of the map follows Oasis montaj protocol.

2.2 Inverting EM61 Data

The EM61 suite of instruments are widely used and accepted by the UXO service providers. Because there are a number of different sensors with slightly different physical characteristics, the first analysis step is to set basic definitions with regard to which EM61 sensor was used to collect the data and how it was configured (Figure 2-1).

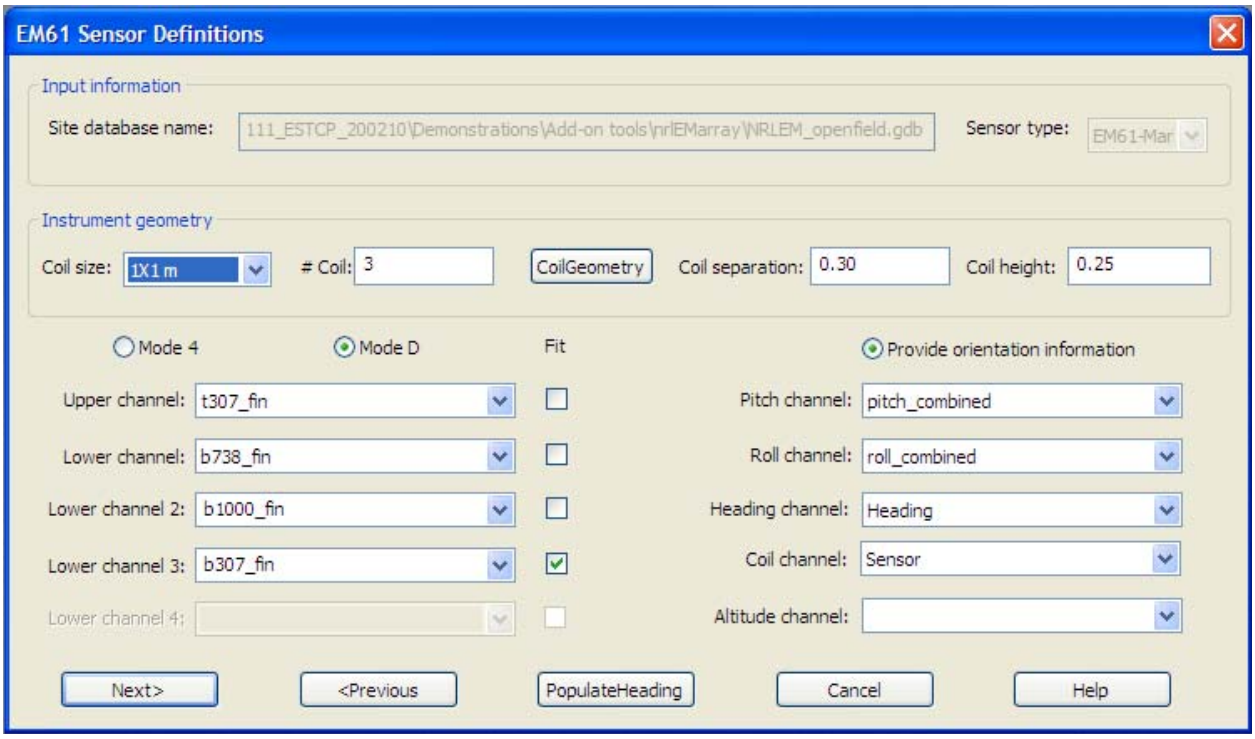

Figure 2-1 Screen snapshot of the 'EM61 Sensor Definitions' GUI.

If the targets have been selected, the inversions can be executed in batch mode. If the targets are being selected in interactive mode, however, users can utilize tools depicted in Figure 2-2. In this figure, the map on the left displays the entire survey area and highlights a portion for analysis (the brighter colors in the bottom left corner of the map). The map on the right focuses on the highlighted portion of the site and provides tools for adding or reviewing anomalies in an interactive manner. Users add new targets simply by clicking on an anomaly using the

Add/Review GUI (right map in Figure 2-2). When a new target is identified, the analysis GUI's in Figure 2-3 are realized.

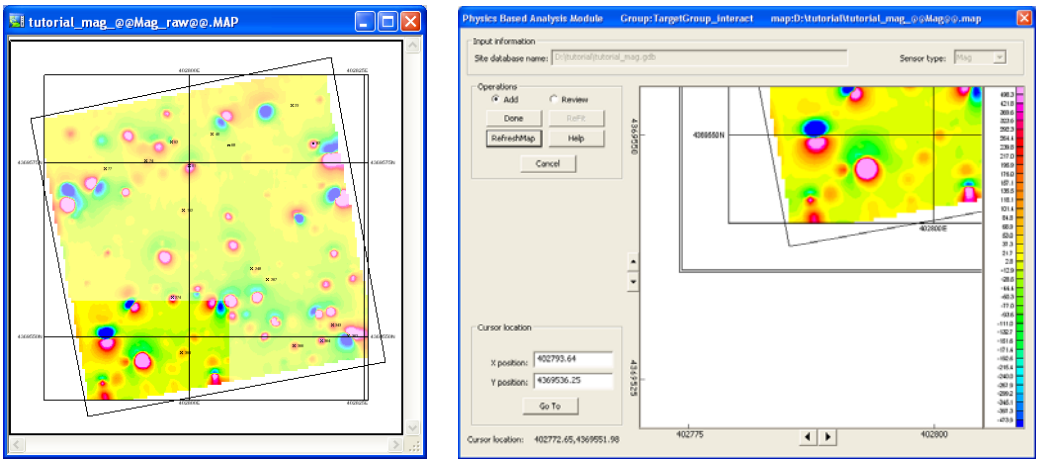

Figure 2-2 Left image: Two dimensional false color map of a survey area. Right image: Screen snapshot showing the 'Add/Review' dialogue of UX-Analyze. This GUI is used to interactively add anomalies or review model results of anomalies that have already been selected and modeled.

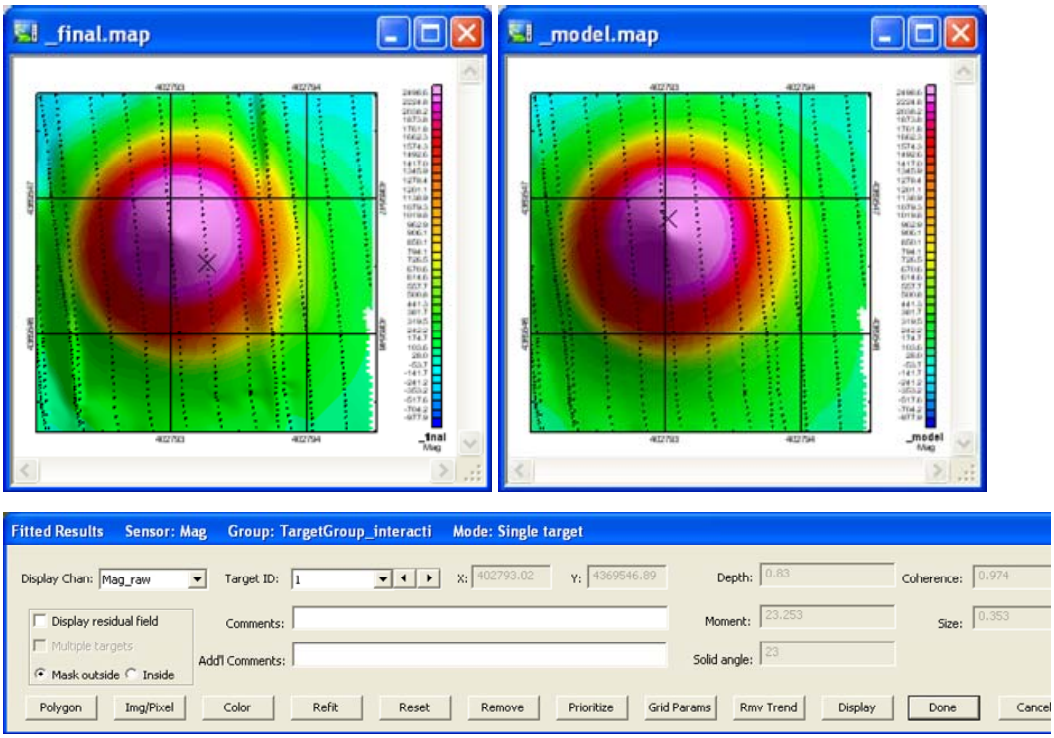

Figure 2-3 Screen snapshot of the 'Fitted Results' GUI. In this multiple-image GUI, the top left map displays the measured data, the top right map shows the modeled data, and the bottom dialogue box displays the inverted parameters.

Once an anomaly is identified, our approach uses a model-based estimation procedure to determine whether or not an unknown target is likely to be a UXO item. It entails estimating the size and shape of the target from the spatial pattern of the induced field above the target. The EMI signal is a linear function of the flux through the receiving coil. The flux is assumed to originate from an induced dipole moment at the target location given by:

$$\mathbf{m} = \mathrm{UBU}^{\mathrm{T}}\mathbf{H}_0$$

where $\mathbf{H}_0$ is the peak primary field at the target, U is the transformation matrix between the coordinate directions and the principal axes of the target, and B is an empirically determined, effective magnetic polarizability matrix. For an arbitrary compact object, this matrix can be diagonalized about three primary body axes. The relative magnitudes of the polarization's are determined by the size, shape and composition of the object as well as the transmit waveform and time gate or frequency. The transformation matrix contains the angular information about the orientation of these body axes.

For cylindrical objects like most UXO, B is a diagonal matrix with only two unique coefficients, corresponding to the longitudinal and transverse directions. Discrimination is based on the target polarizations estimated from spatially mapped data. Specific ordnance items have specific polarization values, while clutter items generally have different principle axis polarizations.

Fitted model parameters include anomaly size (the trace of the polarizability tensor), shape, XY position, depth, orientation, and fit error statistics. In addition to presenting the results of the inversion in spreadsheet form (Figure 2-4), UX-Analyze generates an anomaly summary sheet that shows the measured data, inversion results, and model data for QC purposes.

EMTargets.gdb

TargetGroup_EM61	Fit_Depth	Fit_Size	Fit_b1	Fit_b2
5.0	0.37	0.027	0.1	0.0
6.0	0.46	0.085	3.0	0.3
7.0	0.72	0.083	4.1	0.5
8.0	0.57	0.082	3.1	1.0
9.0	0.35	0.101	4.9	0.0
10.0	0.24	0.086	3.1	0.7
11.0	0.10	0.042	0.3	0.1
12.0	0.68	0.193	49.6	6.3
13.0	0.34	0.020	0.0	0.0
14.0	0.53	0.088	4.8	0.2

Cell 17.0

Figure 2-4 Example EMI target database showing some of the inverted fields; including depth, size, and some of the principle axis polarizations (viz., Fit_b1, Fit_b2, etc.)

2.3 Magnetic Data

In addition to EMI modeling, UX-Analyze makes available inversion routines for magnetic data. Similar to EMI, the first step is to establish a few sensor definitions and site parameters (Figure 2-5). Once the sensor definitions are established, targets need to be selected – either interactively as described above, or imported from a list of target that has been previously generated.

For magnetic data, our model is a simple magnetic dipole. Experience has shown that if the source of the anomaly is metallic, compact, and sufficiently far from the sensor, the dipole term dominates.

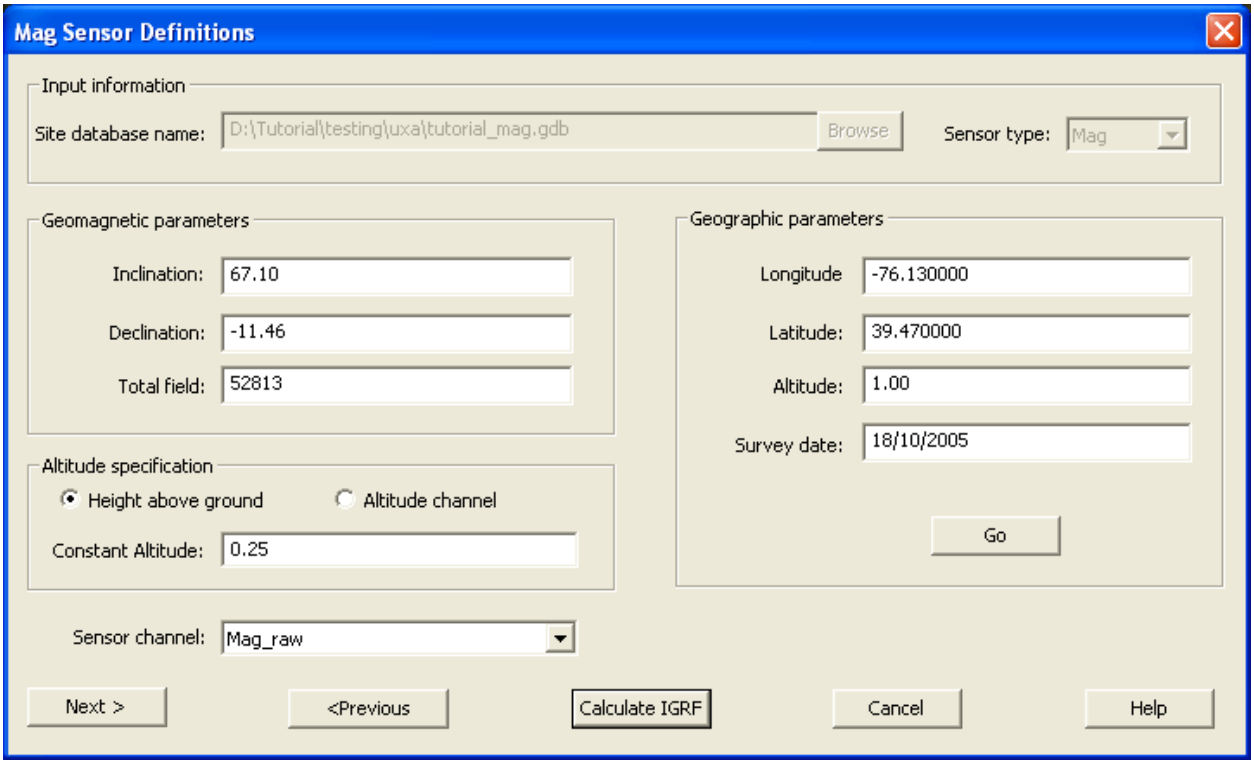

Figure 2-5 Screen snapshot of the 'Mag Sensor Definitions' GUI.

Once the setup parameters are completed and the targets are selected, the anomalies are sequentially inverted. Figure 2-6 shows the magnetic analysis environment during inversions. Target location, depth, and the strength of the magnetic dipole (a size related attribute) can be estimated from magnetometer survey data. Similar to the EMI case, the inverted model parameters are then stored in a database and viewed using native Geosoft tools or exported (Figure 2-7).

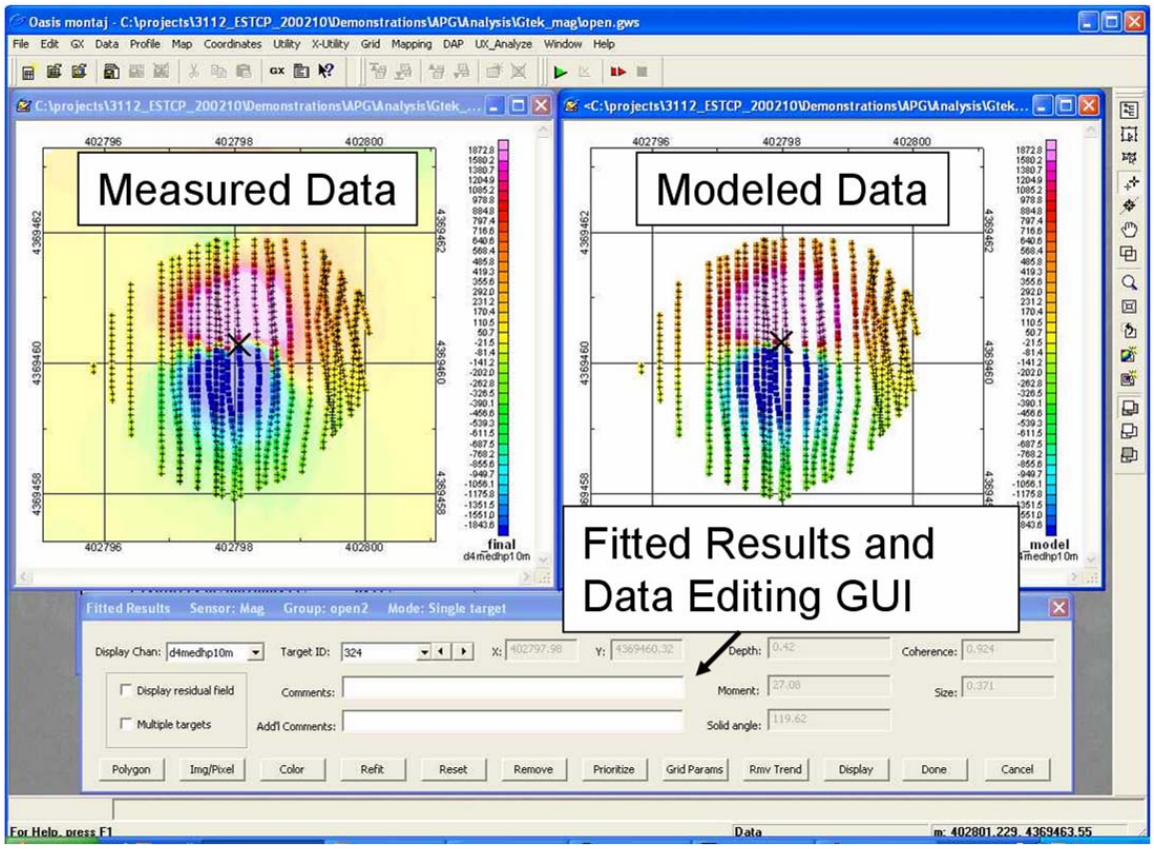

Figure 2-6 Screen snapshots showing the magnetic user interface during data inversion. The measured data is shown in the upper left map, the model parameters in the lower center window, and the forward model generated using the model parameters is shown in the upper right map.

MagTargets.gdb

TargetGrd	Target_ID	utm_x	utm_y	Fit_X	Fit_Y
0.0	1	402796.60	4369581.96	*	*
1.0	2	402818.67	4369583.71	*	*
2.0	3	402791.16	4369579.22	*	*
3.0	4	402797.31	4369577.98	*	*
4.0	5	402799.72	4369576.40	*	*
5.0	6	402807.75	4369575.55	*	*
6.0	7	402819.98	4369576.15	*	*
7.0	8	402790.59	4369570.81	*	*
8.0	9	402818.80	4369571.85	*	*
9.0	10	402799.14	4369568.37	*	*
10.0	11	402799.57	4369566.21	*	*

Chan Target_ID

Figure 2-7 Example magnetic target database showing some of the inverted fields; including, ID number, and XY information.

2.4 Classification Module

Once all of the anomalies have been inverted and target attributes have been generated, the fitted parameters can then be used to classify the unknown targets as either targets of interest, or not, by utilizing a statistical classifier or by using thresholds set using labeled data. With regard to statistical classifiers, the generalized likelihood ratio test (GLRT) has been incorporated into the UX-Analyze framework. Although the mathematics behind the classifier is non trivial, the implementation is rather straightforward. Figure 2-8 presents the classification GUI. In addition to specifying the name of the target database and specific channels (or fitted parameter), the user must specify the name of the database containing the labeled data.

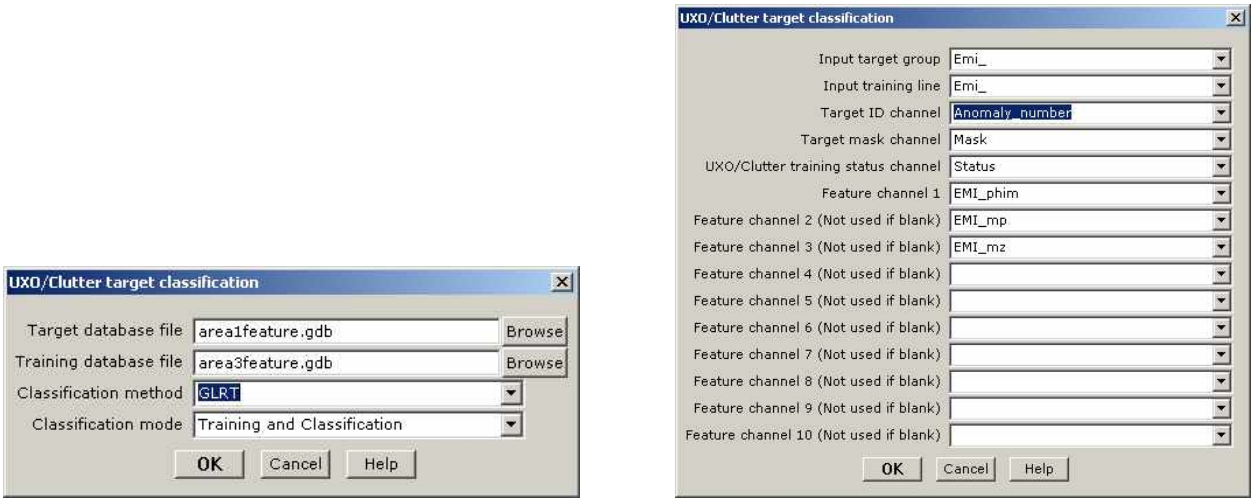

Figure 2-8 Screen snapshots showing the user dialogue interfaces that call the GLRT classification routines.

2.5 Data Analysis Documentation

Once the characterization and classification steps have been completed, UX-Analyze can be used to produce individualized anomaly reports to document the decision process. In each of the anomaly summary plots, the measured data is graphically displayed next to the modeled data. The model parameters are listed in the middle of each page, and a profile extracted along the transect that passes closest to the dipoles location – as estimated by the inversion routine – is located at the bottom. The positions of individual measurements are superimposed on the maps (Figure 2-9).

Essentially, the anomaly plots graphically provide an intuitive confidence measure. If the measured and modeled data are indistinguishable, the reviewer can have confidence that the estimated source parameters are approximately correct. If the two maps are do not resemble each other, however, it tells us that the source in question (i) cannot be represented well using a point dipole source, (ii) is not isolated, (iii) does not have sufficient signal-to-noise ratio, or (iv) was not properly sampled (spatially or temporally). In any case, if the two maps are dissimilar the inverted target attributes are most likely not meaningful.

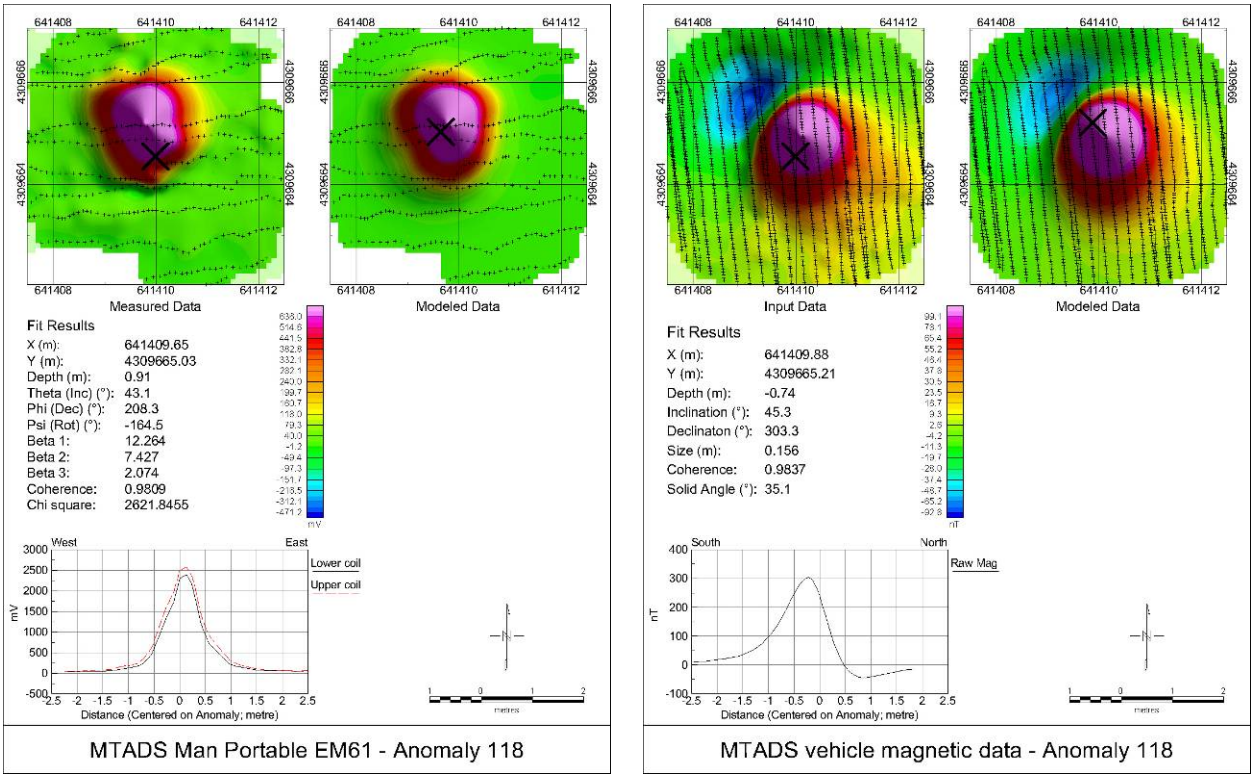

Figure 2-9 UX-Analyze generates a one-page summary for each anomaly. EMI data are shown in the left summary, and magnetic data on the right.

2.6 Factors Affecting Cost and Performance using UX-Analyze

The analysis approach demonstrated here utilizes the spatial distribution of the measured magnetic or EMI signatures. As such, it requires high signal-to-noise data that possess a high degree of spatial precision across the footprint of the anomaly. The costs to acquire data that will support discrimination decisions are higher than that required if the goal is only to detect the presence of an object. The analysis costs associated with discrimination decisions are also higher than detection alone.

The factors affecting acquisition costs relate to particulars of the sensing system, spatial registration system, the target objectives, and the site environment. Although these costs are not the focus of this demonstration, they are very important to the ultimate transferability of this approach.

The factors affecting analysis time include are significantly affected by (i) the degree to which the anomalies are spatially separated, (ii) the number of anomalies, and (iii) the amount of geologic-related signatures that possess similar wavelengths as the targeted signatures. The data density is also a factor, but only marginally so compared to the factors listed above.

Discrimination performance is measured by our ability to characterize and classify one object from another. The factors that affect performance, therefore, relate to the similarity (in feature space) between the sought-after object versus the clutter, our ability to accurately measure the responses, the presence of signatures that spatially interfere or otherwise compete with the UXOs response, as well as our ability to quantitatively characterize and classify the source objects. Many of these factors are not under our direct control.

Implementation of the demonstrated analysis method requires additional time compared to that required for detection only. This is because the analyst must not only identify and locate the anomaly, but also must extract signal responses while excluding background or overlapping signatures to the extent possible, re-level the extracted data if needed, and invert data around the anomaly for model parameters.

2.7 Advantages and Limitations

This technology uses spatially referenced geophysical data to estimate target features using a dipole model. This has an inherent advantage over non-quantitative or less robust methods. Ancillary analysis methods sometimes include metrics such as the anomaly amplitude, half width, spatial footprint, or overall ‘look’. These later metrics are, however, sensitive to the targets’ orientation and depth of burial. The methodology demonstrated here separates the measured signatures into that which is inherent to the target, and that which is related to the geometry of the problem (such as distance to sensor and orientation).

The primary advantage, therefore, is the potential for discriminating between UXO and non UXO-like objects based upon geophysical survey data. This is in contrast to simply identifying

the location of anomalies from the geophysical survey data. Magnetic classification is often based primarily on the apparent fitted dipole size (or scaled dipole moment). Using EMI data, increased classification performance can sometimes be achieved by utilizing estimated shape information that is contained in the principle axis polarization values. If successful classification capabilities are realized, significant savings can be realized by leaving the non-hazard clutter items unearthed or by changing the remediation protocols to less costly measures depending on the classification.

Known limitations to the data analysis approach adopted here result from (i) non-unique inversion results, and (ii) overlapping, or non distinct, signatures in feature space. The former limitation, one in which multiple sets of model parameters explain the vast majority of the observed data, is well known. The second, while perhaps not as widely appreciated, is equally problematic. Inverting EMI data using our dipole models, results in three eigenvalues of the magnetic polarizability tensor, each corresponds to a principal axis of object. Classificaiton is possible only to the degree that the derived eigenvalues are different for different objects and stable for similar classes of objects. In other words, even with ideal data, the estimated burial depth, apparent size, and shape features may not separate UXO and clutter signatures into distinct, non-overlapping classes. This is because the anomaly features derived from EMI and magnetic data are not unique to UXO. Clutter items that have similar shapes and burial attributes to ordnance can have geophysical signatures that are indistinguishable from UXO signatures and, as such, will have similar eigenvalues and therefore likely be classified as ordnance. Examples include items such as pipes, post sections and axial symmetrical fragments.

3. Supplemental Tools and Data Examples

3.1 Inversion of EM61 Array Data

In addition to fitting data acquired using a single sensor EM61, UX-Analyze provides means to properly invert data acquired by an array of EM61 sensors (Figure 3-1). The coil array geometry is entered by depressing the "CoilGeometry" button which realizes another GUI that allows the user to enter the relative positions of each of the coils. After entering the positions of all the coils the user has the option, by selecting the preview button, to create and display a schematic diagram of the EM array based on the user input. After properly entering the array geometry, the inversion routines automatically account for the geometry of the coils.

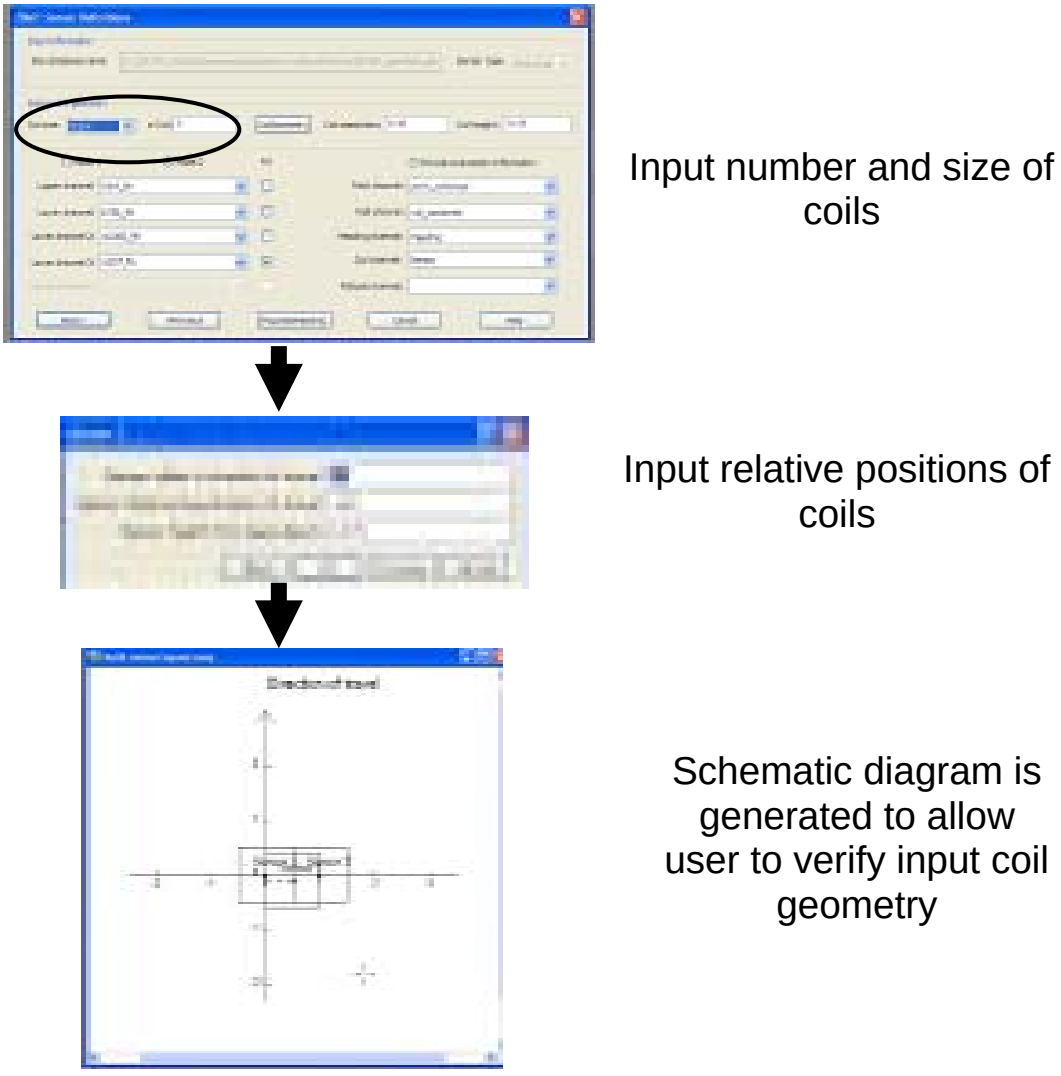

Figure 3-1 Flowchart of user friendly GUI's created in UX-Analyze to input the coil geometry of EM61 arrays.

3.1.1 Algorithm Equivalence

Algorithm equivalency tests verified that the C-based inversion routines embedded in Oasis montaj produce identical performances as the original formulations. The original inversion routines, were previously developed by SAIC (formerly AETC Incorporated) for the *MTADS* Data Analysis System (DAS) under funding from ESTCP and SERDP. The MTADS DAS codes were prototyped using the Interactive Development Language (IDL) and hard coded to invert the MTADS EMI array sensor data. The EM61 MkII MTADS array is an overlapping array of three pulsed-induction sensors specially modified by Geonics, Ltd. based on their EM61 MkII sensor with 1m x 1m sensor coils.

To ensure that each routine received the exact same input for each anomaly, we extracted data samples around 18 isolated targets from Aberdeen Proving Ground. The extracted anomaly data were then inverted using the two inversion routines and compared. Figure 3-2 to Figure 3-4 compare the fitted parameters output form the two inversion routines. It is clear from these figures that the results are equivalent.

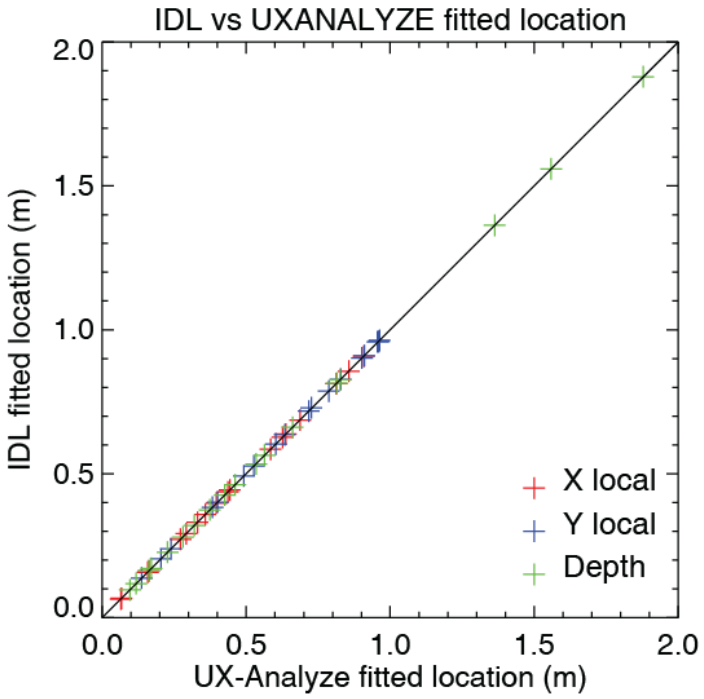

Figure 3-2 Comparison of Fitted location using UX-Analyze and IDL; electromagnetic data.

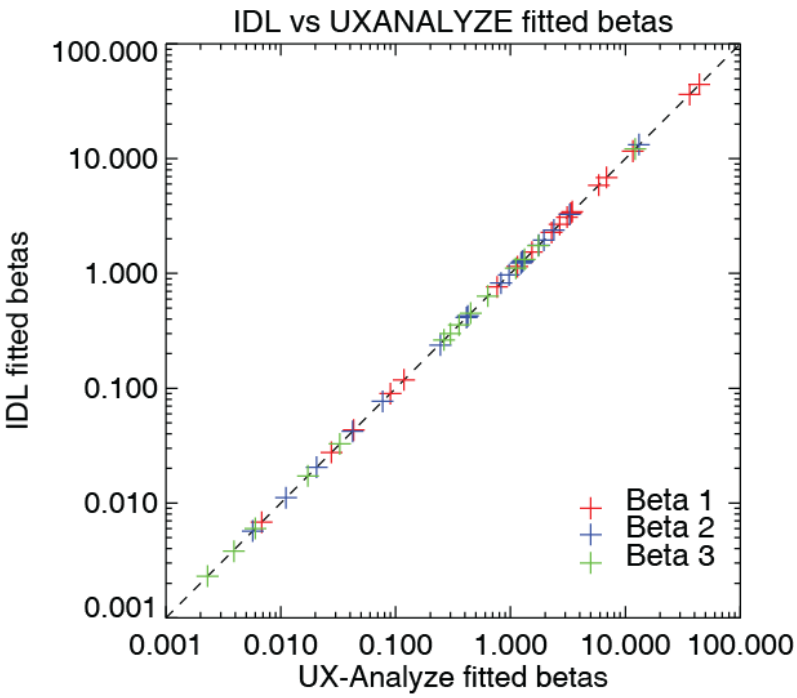

Figure 3-3 Comparison of Fitted Betas using UX-Analyze and the DAS; electromagnetic data

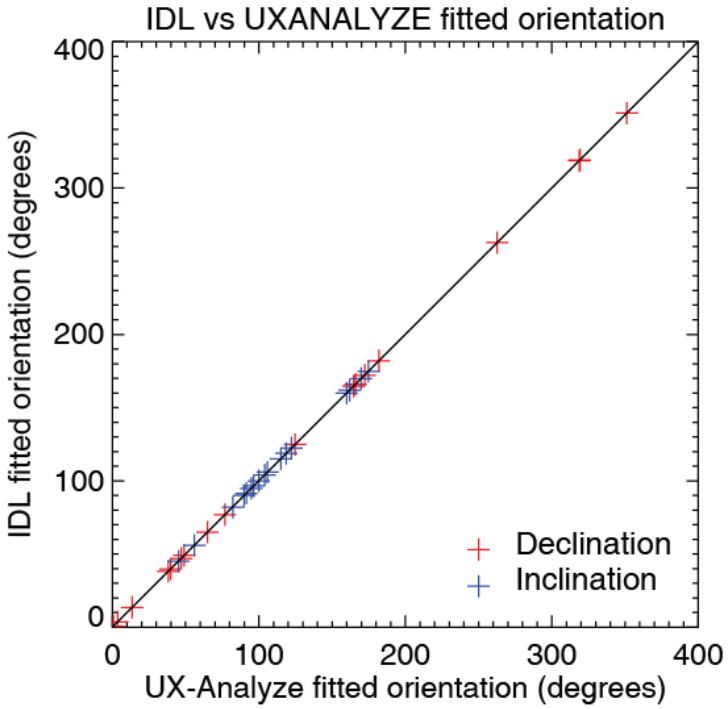

Figure 3-4 Comparison of Fitted dipole orientation using UX-Analyze and the DAS; electromagnetic data

3.2 Multi-channel Data Leveling

3.2.1 Description of Test Data

The EM63 data acquired by ERDC at the blind grid at the Aberdeen Proving Ground Standardized Test Site was used to demonstrate auto-leveling routines. The EM63 is a commercially available sensor produced by Geonics, Ltd., of Mississauga, Ontario, Canada. It is a high power, high sensitivity, wide bandwidth full time domain UXO detector. The EM63 consists of a transmitter that generates a pulsed primary magnetic field which induces eddy currents in nearby metallic objects. The time decay of the currents is measured and recorded by the main console at 20 to 30 geometrically spaced time gates covering a time range from 180 microseconds (μs) to 63 milliseconds (ms).

The EM63 system consists of three major hardware subsystems: (i) EM63 Control Console Sub-System; (ii) Antenna Cart Sub-System; and (iii) GPS Navigation Sub-System. The EM63 Control Console Sub-System consists of receiver and transmitter unit, controlled by an integrated field computer. The Antenna Cart Sub-System consists of the transmitter antenna (the 1x1m bottom coil) and receiver coils. Local positioning and georeferencing was accomplished using a Trimble 5700 real time kinematic (RTK) GPS system. The Trimble system consists of two receivers that are in radio communication with each other. A roving GPS antenna is mounted in the center of the EM63 coils and 2 meters above the bottom coil. The operator or assistant carries the controller for the roving antenna.

3.2.2 Graphical User Interface for EMI Array Inversion

The GUI to the data leveling routines in UX-Analyze is shown in Figure 3-5. The routine has the option to level multiple channels which is very useful for leveling the 26 time gates output from the EM63 sensor. The input channels are selected from a drop down list and output channels containing the leveled data are automatically created by adding a suffix corresponding to the leveling method to the input name. There are three leveling methods available. The three methods named Mean, Minimum and Mode require input parameters for the measurement and change window size for distance and time. The Mode option also requires a triangle size and bin size which are used to increase the robustness of the mode calculation by convolving the histogram with a triangle N units high and 2N-1 bins wide.

In general the mode option works well if there is sufficient background between target anomalies to dominate the mode in the defined windows. For areas with high densities of anomalies the minimum option works better as long as the data do not contain any negatives spikes. The mean option is used when there are relatively equal numbers of positive and negative anomalies in the data.

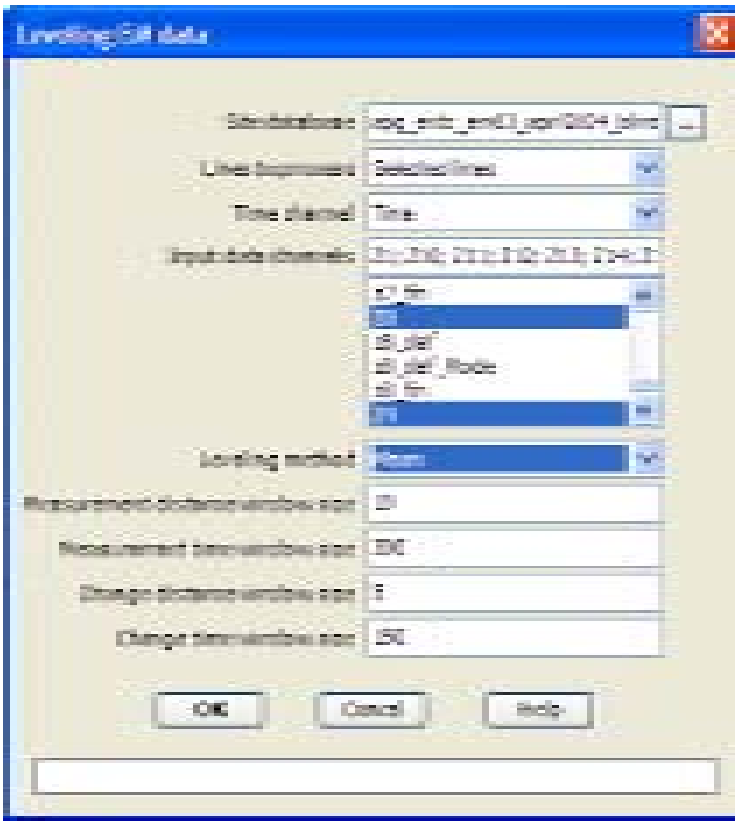

Figure 3-5 Input dialog for data leveling routines.

3.2.3 Data example

Figure 3-6 illustrates the process that was applied to the APG blind grid EM63 data. The EM63 data consists of 26 channels of lower coil data and 1 upper coil channel. The figure shows the data for the lower coil 1st time gate. The raw EM63 data (red profile) was plagued by a data spike at the beginning of each line. The spike was located at the 2nd or 3rd point of each line and occurred on the majority of the data channels. The spike was removed by simply deleting the first three records of each line. This method had no detrimental effect on the survey coverage because the sensor was stationary and located outside the grid. The large positive spikes in the data would not create problems when using the mode or minimum leveling options but would cause problems with the mean option. The despiked data channel (green profile) was input to the leveling routine and the mode method was selected.

The autoleveling routine divides the data into windows and calculates and applies a correction for each window resulting in a leveled data channel (blue profile). A drawback to this method is the formation of small steps in the data caused by discrete differences in the corrections calculated for each bin or window. These are easily seen in middle panel of Figure 3-6 by the magenta profile which is produced by subtracting the leveled channel (blue profile) from the input channel (green profile). These steps are easily removed by applying a B-spline filter to the correction channel (magenta profile) which results in the smoothly varying final correction

channel (cyan profile). This final correction channel is added to the original data giving the final leveled channel (cyan profile) in the lower panel.

The effects of the leveling routines are clearly evident in gridded images. Figure 3-7 presents mapped EM63 data acquired at the APG blind grid area. We plot on the left hand side the original unleveled data and leveled data on the right using the same color scales.

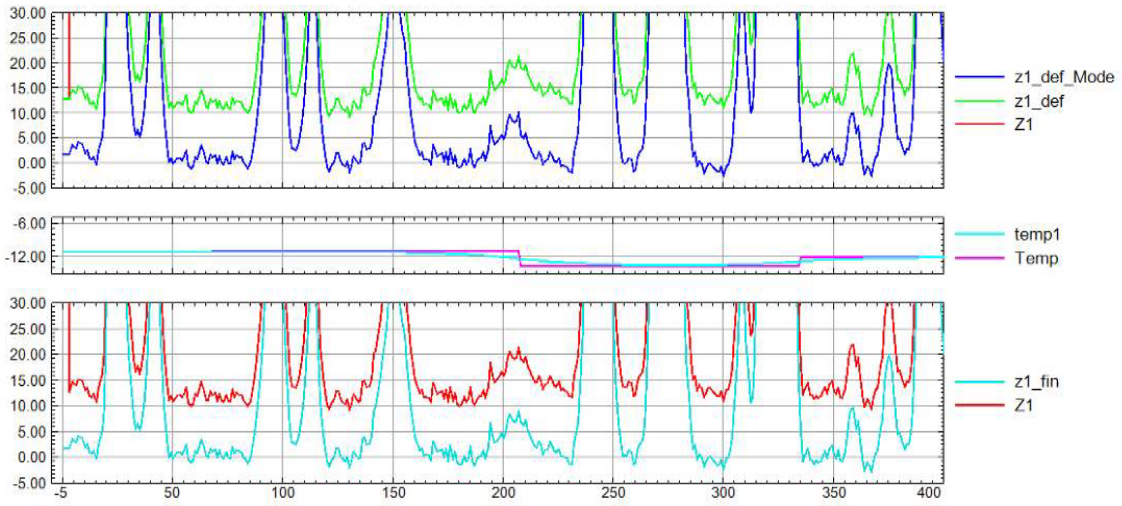

Figure 3-6 Profile plot showing the 1st time gate and intermediate leveling channels for a line of EM63 data from the blind grid at APG.

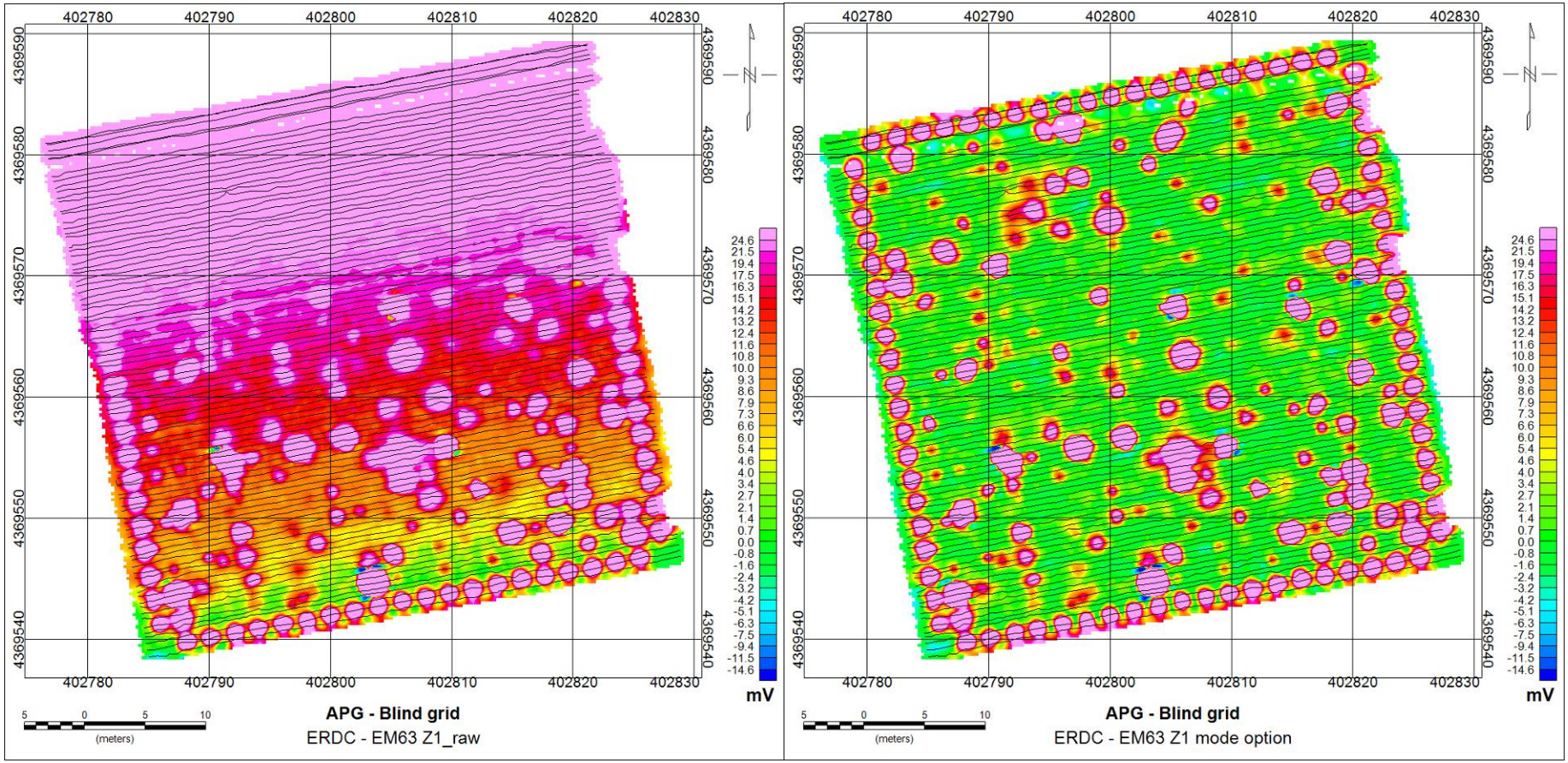

Figure 3-7 APG blind grid data (1st time gate) before (left) and after leveling (right).

3.3 Magnetic Soil Analysis

3.3.1 Description of Test Data

To demonstrate the magnetic soils discrimination algorithm, we used EM63 data collected over the test grid at Blossom Point. These data were collected in January 2004 in support of ESTCP project MM-0326. These data were collected using the standard man portable cart and positioned using GPS. The Blossom Point test grid is 30x100m in size and is comprised of six lanes with 15 potential targets in each lane spaced 6m apart. The items buried in the test grid include inert ordnance, ordnance simulants, test shapes and representative clutter at a variety of depths and orientations. We will concentrate our analysis on lane Z which consists of 60mm mortars buried at various depths and orientations. Figure 3-8 shows a color contour map of the EM63 1st time gate channel over lane Z at the Blossom Point test bed. The anomaly at the north end of the lane is cause by an aluminum sphere that was placed on the ground.

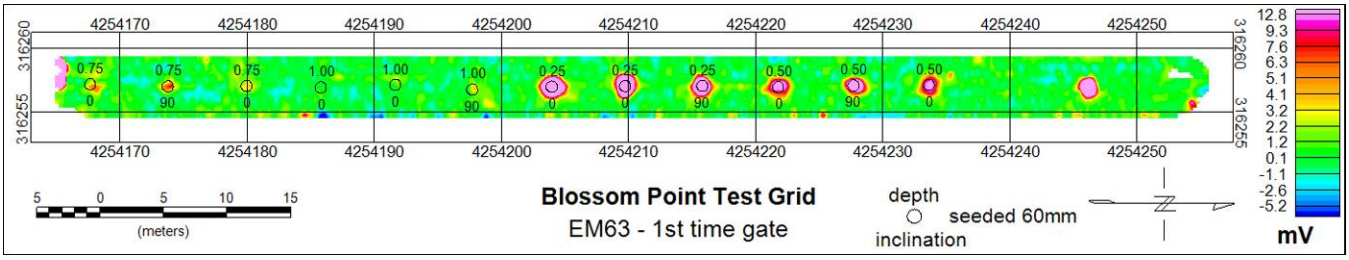

Figure 3-8 False color images showing EM63 data (1st time gate) over lane Z of the Blossom Point test grid. The symbols identify seeded 60mm mortars.

We also used EM61 MarkII cart data collected over the southwest area at Camp Sibert. These data were collected in support of the ESTCP discrimination study in 2007. According to the ground truth from the southwest area, the source of many anomalies were soils or rock. This provided a good test to measure the effectiveness of the soil/metal chi square discrimination algorithm using an EM61 recording three time gates covering a time range from 214 microseconds (μs) to 660 microseconds (μs). Figure 3-9 shows the 0.214ms lower coil data recorded from the EM61 cart over the southwest area at Camp Sibert. The symbols represent different categories of ground truth with the red circles indicating anomalies caused by rock or soil and the different black symbols show anomalies caused by a metal object.

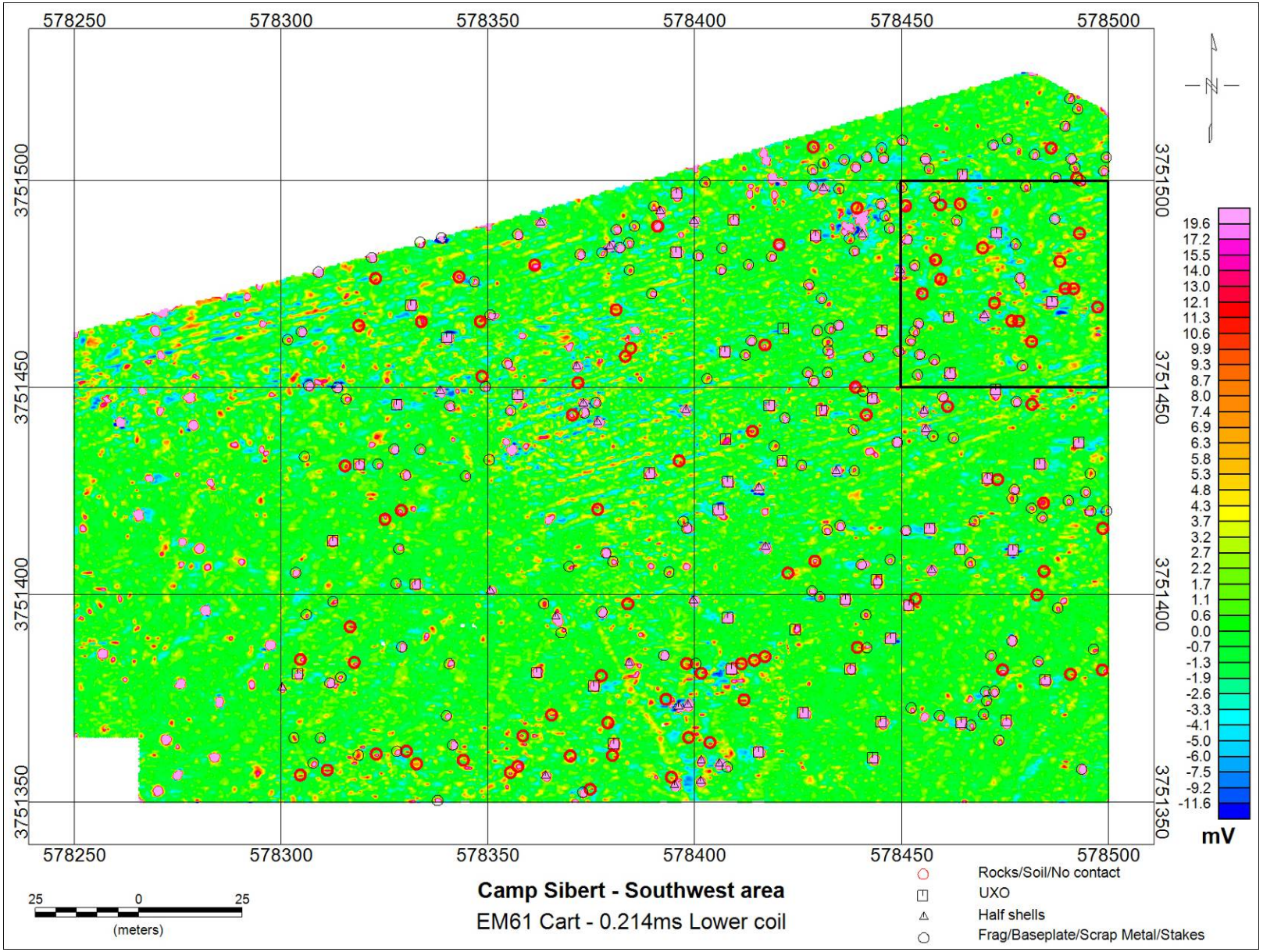

Figure 3-9 False color image showing the EM61 0.214ms time gate lower coil data over the southwest area at Camp Sibert.

3.3.2 Graphical User Interface for Soil-Metal Discrimination analysis

The GUI to the soil-metal discrimination algorithm in UX-Analyze is shown in Figure 3-10. The input parameters are very similar to those for the automatic leveling routines described in the previous section. The input channels are selected from a drop down list and output channels are automatically created by adding the suffix "_discrim" to the input channel names and a "Chisq" channel is created that contains the Chi square error of the "_discrim" data that was fit to either the default magnetic soil model or a user defined magnetic soil model. The Chi square will produce peaks where the sensor response did not match the soil model and presumably caused by a metal object.

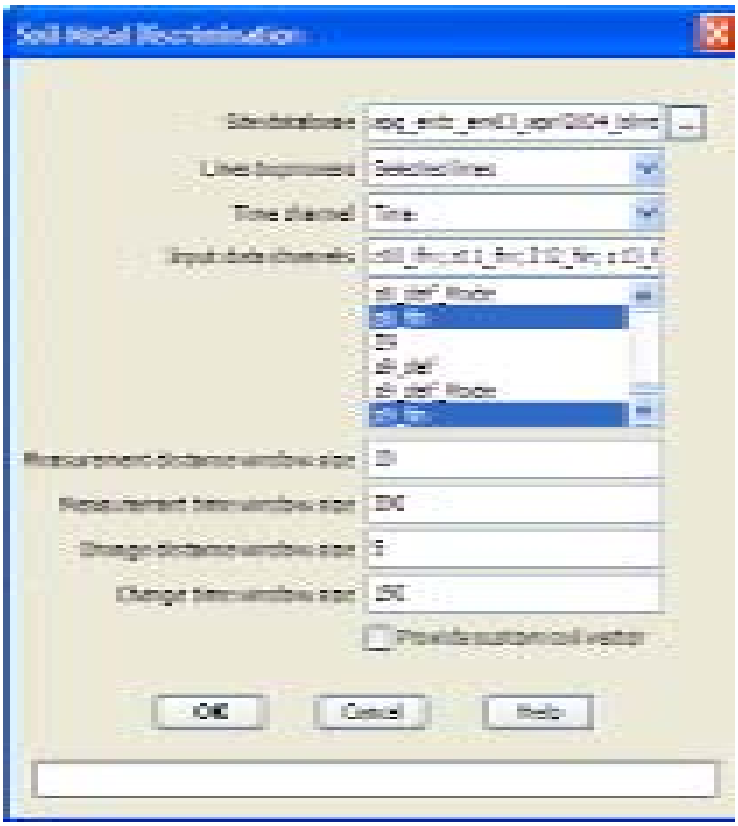

Figure 3-10 Input dialog for soil – metal discrimination algorithm.

3.3.3 Data example

Figure 3-11 shows the results of the soil/metal discrimination algorithm. The top panel shows the Chi square profile and the bottom panel shows the output leveled lower coil data for a few time gates. The profile shows data collected from north (left side) to south (right side) along the line closest to the center of the seeded mortars. The chi square profile clearly shows a peak at the same location as the peaks in the lower coil profiles which correspond to a metal object (60mm mortar or aluminum sphere). Unfortunately, the Blossom Point test grid did not contain any anomalies caused by geology to test the effectiveness of removing geologic anomalies.

Figure 3-12 shows Chi square output over the lane Z of the Blossom Point test grid as a false color image.

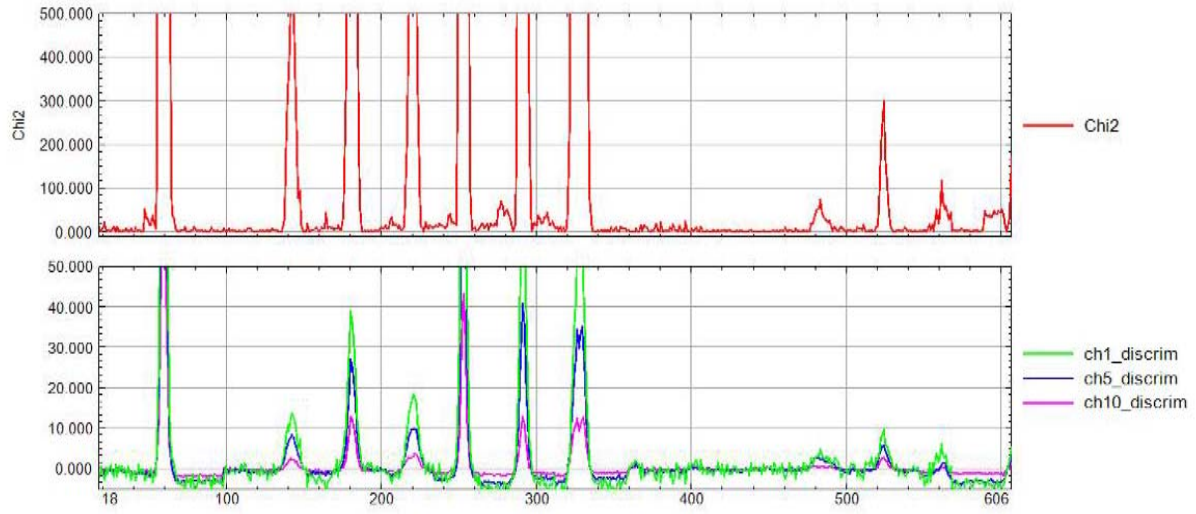

Figure 3-11 Profile plot of data collected along a line directly over the emplaced 60mm mortars. The horizontal scale is fiducial based with 1 fiducial representing 0.1 seconds. The profile was collected in the north-south direction.

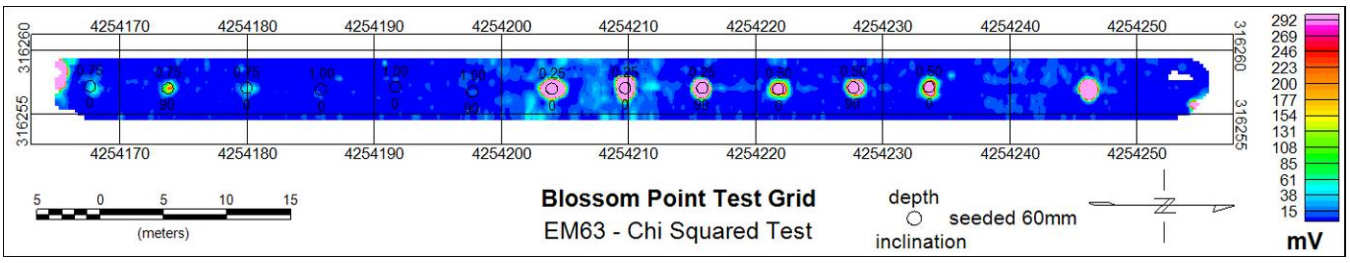

Figure 3-12 False color image showing the Chi squared analysis over lane Z of the Blossom Point test grid.

Figure 3-13 shows the Chi square output for the EM61 cart survey over the southwest area at Camp Sibert. The red circles plot anomalies associated with rocks or soils. The black symbols represent anomalies caused by a metal object and should correspond to a peak in the Chi square output. The east-west anomalous features in the Chi square figure are artifacts caused by the automatic data leveling built into the soil/metal algorithm. Comparing Figure 3-9 to Figure 3-13 we clearly see the overall effect of geology (evidence by the southwest-northeast linear anomalies in the EM61 data) is greatly reduced in the Chi square map. On closer inspection at the individual anomalies we see that most anomalies associated with a metal object also correspond to a Chi square anomaly. In addition many of the anomalies that were caused by rock or soil have been suppressed or eliminated from the Chi square map.

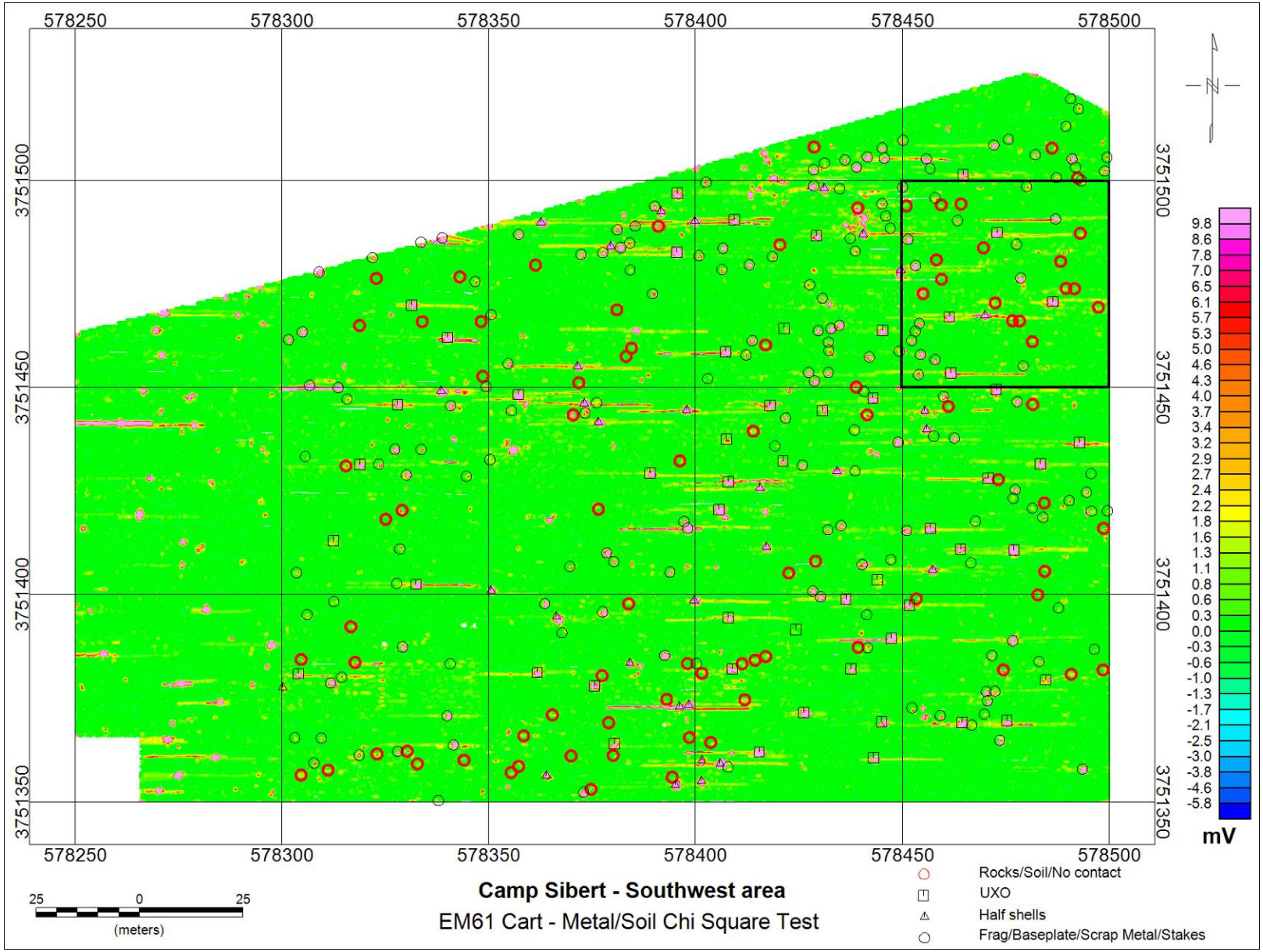

Figure 3-13 False color image showing the soil/metal chi square output over the southwest area at Camp Sibert.

Figure 3-14 shows a comparison of the EM61 lower coil data and the Chi square output over a portion of the southwest area indicated by the black box in the northwest corner of Figure 3-13. This section of data contains examples of anomalies associated with geology being eliminated but also some that still contain an anomaly in the Chi square. We also see that most of the anomalies caused by a metal object (black symbols) also show a peak in the Chi square but there were a few anomalies along the western and northern edge that do not.

In general the soil/metal algorithm does show some promise but the elimination of some anomalies caused by a metal object is troublesome. Improvement to the method may be achieved if the EM61 were programmed to collect four time gates of data instead of three gates and the top coil. The addition of the later time gate may capture enough of the time decay to improve the performance of the algorithm. Even better would be using the EM63 because its time decay extends to 63 milliseconds (ms). Improvements may also be made by using a soil vector that was customized to the site instead of the default soil vector.

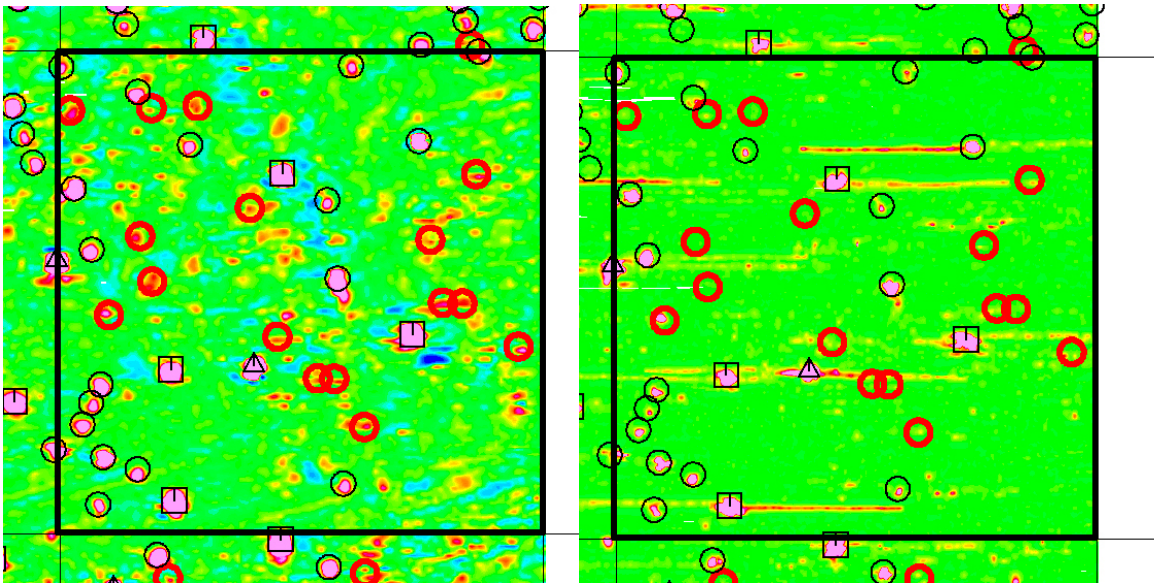

Figure 3-14 False color images of .214ms lower coil data (left) and chi square output (right) of a portion of the southwest area (black box in Figure 3-13). The color scales and symbols are the same as Figure 3-9 and Figure 3-13.

3.4 Inversion of EM63 data using modified POB model

3.4.1 Description of Test Data

To evaluate the EM63 inversion routines, we leveraged data collected by the Naval Research Laboratory at Blossom Point as part of the overlapping signatures database. The measurements were collected in cued mode using a 2x4 meter grid. The grid had a lane spacing of 25cm and a down-track sampling of 10cm near the center of the target and 20cm elsewhere (Figure 3-15). Figure 3-16 shows the four different types of ordnance that were used (40mm, 60mm, 80mm,

and 105mm). Each of the targets was measured individually, with the ordnance measured in three orientations (horizontal, vertical with nose up, and vertical with nose down).

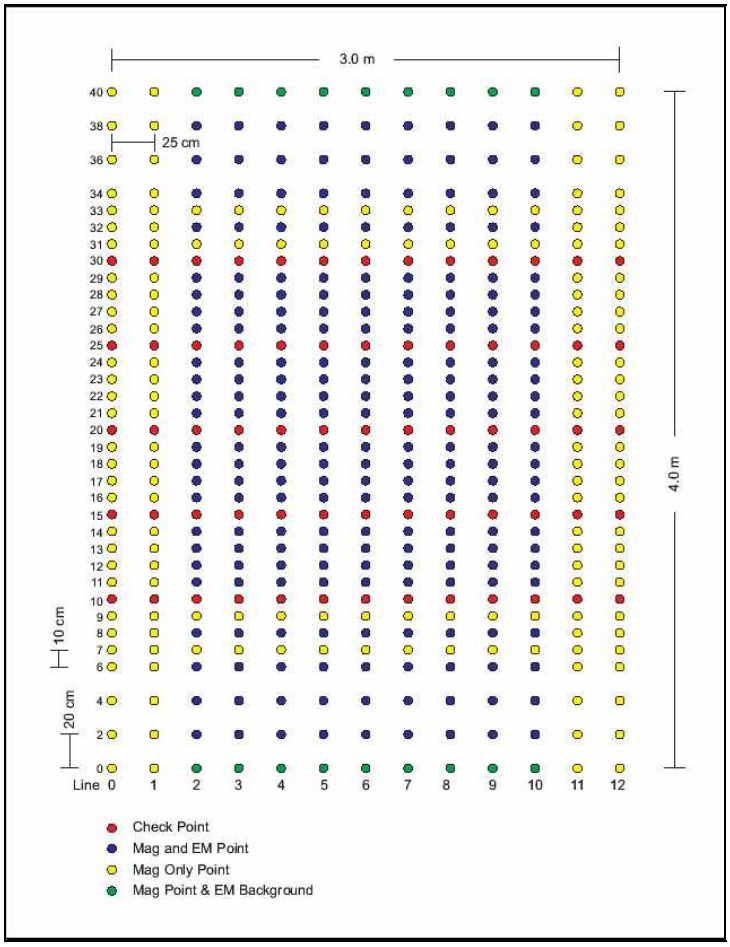

Figure 3-15. Data measurement locations for EM63 cued data collection at Blossom Point.

Figure 3-16 Picture of the four types of ordnance measured. Starting on the left is a 105mm projectile, an 81mm mortar, a 60mm mortar and a 40mm M385.

3.4.2 Modifications to POB model and GUI for EM63 Inversion

The full Pasion-Oldenburg-Billings (POB) analysis assumes an axially symmetric (axial and transverse) tensor dipolar target response, and solves for the best fit of 13 parameters; six intrinsic (Ki, Bi, Gi), five extrinsic (x, y, z, azimuth, inclination), and the two 'time shift' parameters (Ai). The time dependence (proposed by Duncan McNeill of Geonics Ltd.) is of the form:

$$F(t) = (\text{Geometric Factor}) * Ki \ (t - Ai)^{-Bi} \ \exp(-t/Gi)$$

(t in msec, i = 1,2 are the axial and transverse responses.)

The POB algorithm that has been incorporated into UX-Analyze has the modifications described below.

The algorithm has been modified to allow an input target depth if available. If not available the algorithm starts with a zero initial depth estimate, which seems to converge much better to the global best fit minimum that using a depth estimate calculated from the top coil to bottom coil ratio.

The Gi parameters (time constants of late exponential decay) would have diagnostic value (for UXO discrimination), but are difficult to determine in typical EM63 data sets because the late gates are often 'in the noise'. In fact, the inversion often returns negative Gi time constants, in order to 'fit' the late gate noise floor. The 'time shift' parameters (Ai) contribute a slight rounding (concave down for negative Ai) in the early log-linear decay which is often observed in field data. However, it is not clear whether this is due to an EM63 timing problem, to unequal amplitude response across the early gates, or to an intrinsic target property. The possible diagnostic value of the Ai is unclear. For these reasons, and to reduce the dimensionality of the

modified Nelder-Mead Simplex minimization from 13 to 9 parameters, we have constrained Ai = zero and the inverse of Gi = zero in the current POB module.

Figure 3-17 shows the input GUI to invert EM63 data using the modified POB algorithm that was integrated into UX-Analyze. The modified version is invoked using the radio button for "GPA-POB". The only inputs required are the EM63 input channel and an altitude channel. There is an option to provide sensor orientation information, if available. The remaining parameters are set to default values.

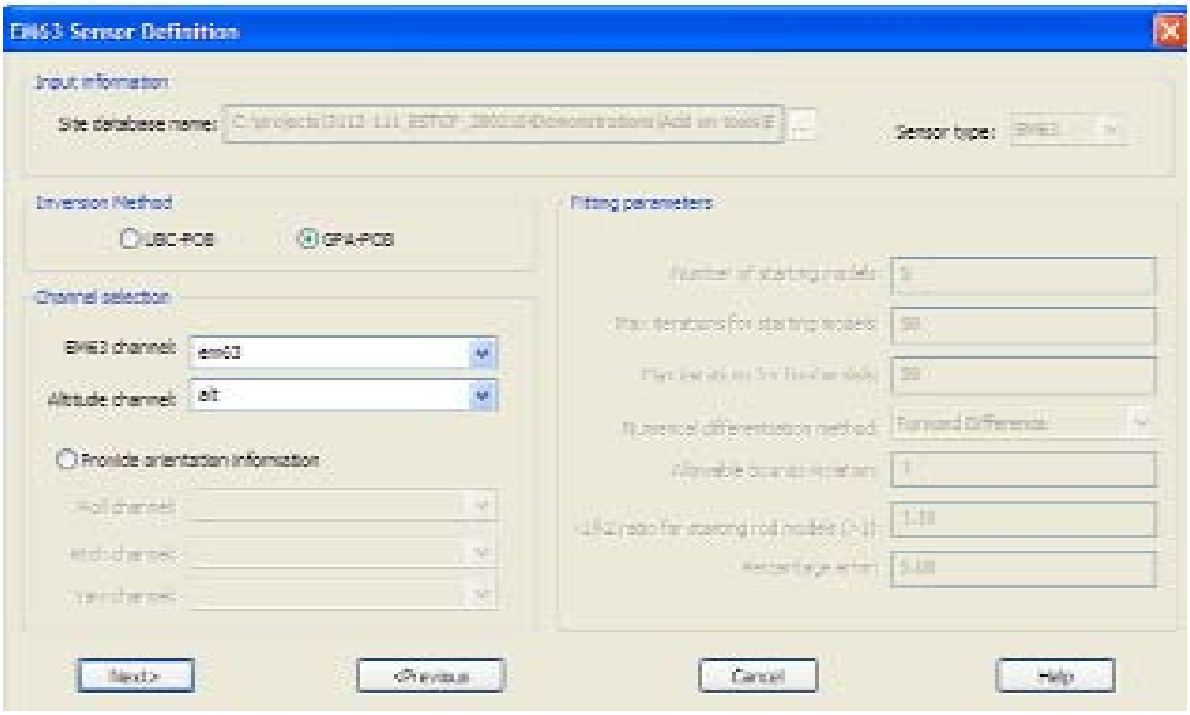

Figure 3-17 Input GUI for EM63 inversion using the modified POB algorithm.

3.4.3 Data example

The EM63 inversion routine completed on the 12 cued data sets (4 targets with 3 orientations) without incident. The targets were fit in batch mode because on average each target took three to four minutes for the inversion to complete. This is a substantial improvement on the ~15 minutes required on the version prior to the modifications made to the algorithm during the integration into UX-Analyze.

The fit coherence, which is the squared correlation coefficient between the measured and modeled data for the 1st time gate, for all the targets except the 40mm nose down was greater than 0.995. The 40mm nose down target contained noisy data for several of the time gates which resulted in the lower coherence. Several of the other targets also contained a number of data spikes and sensor noise for some of the time gates which could account for some of the errors in the fitted parameters. Figure 3-18 presents a comparison of the depth output from the inversion algorithm and the actual depth to the middle of the target. Figure 3-19 to Figure 3-24 show a

color image of the measured and modeled data as well as the fit parameters for each of the targets analyzed. In general, ferrous objects should have an average beta value > 0.8 with the ratios K1/K2 >1 and B1/B2 <1 for rod-like objects. For non-ferrous objects, the ratio K1/K2 <1 indicates the target is rod-like[1].

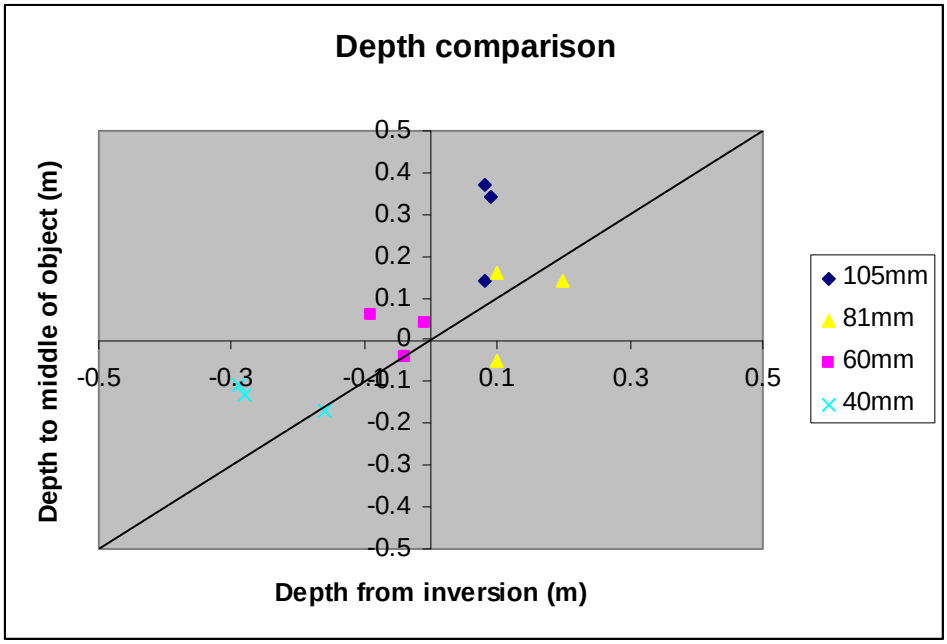

Figure 3-18 Comparison of the actual depth versus the depth output from the EM63 inversion.

[1] Pasion, L.R., and Oldenburg, D.W., 2001, Locating and determining dimensionality of UXO using time domain electromagnetic induction, Journal of Environmental and Engineering Geophysics, v6, p91-102.

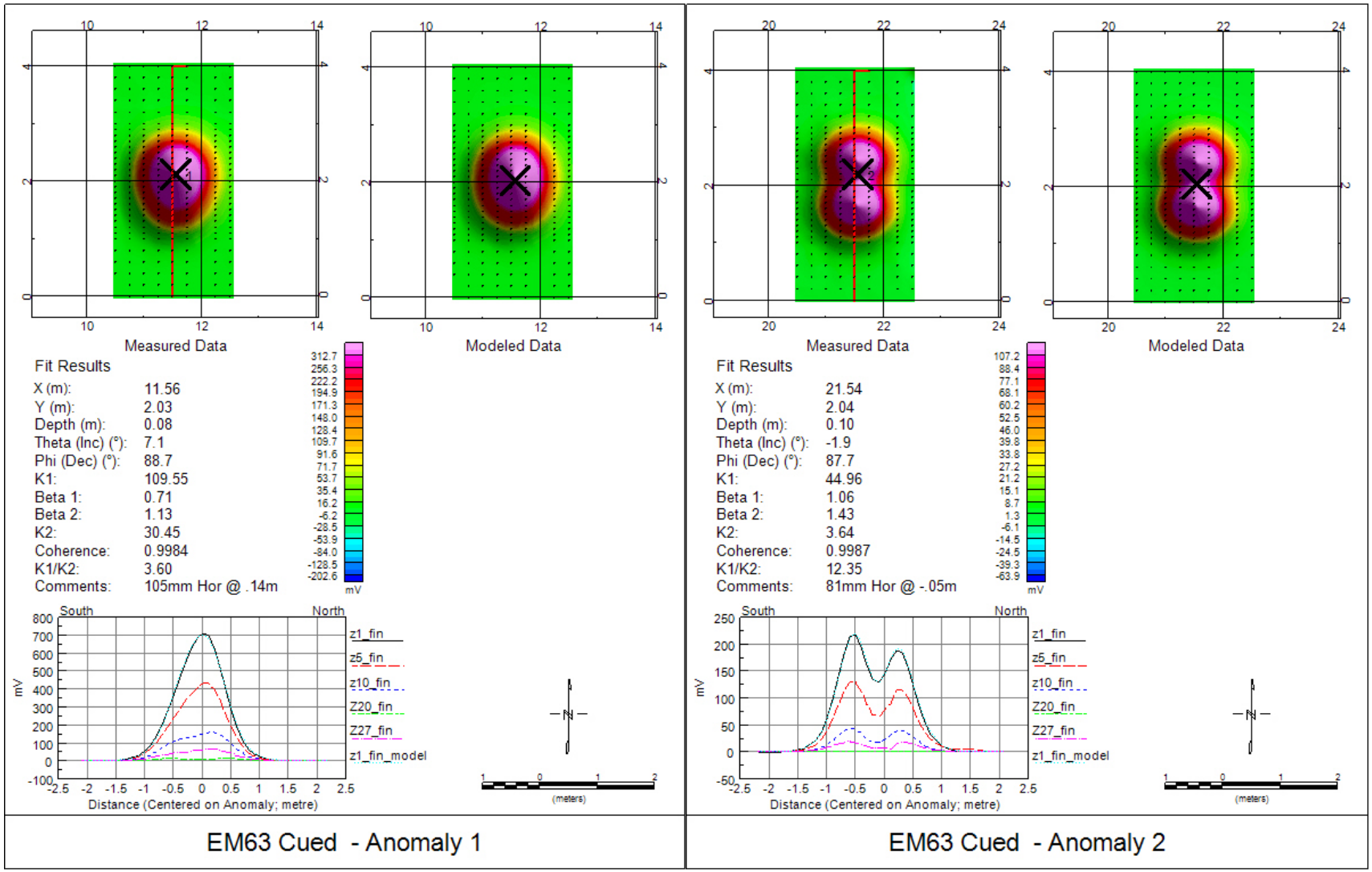

Figure 3-19 Anomaly plots of EM63 inversion results for 105mm (left) and 81mm (right) in a horizontal orientation.

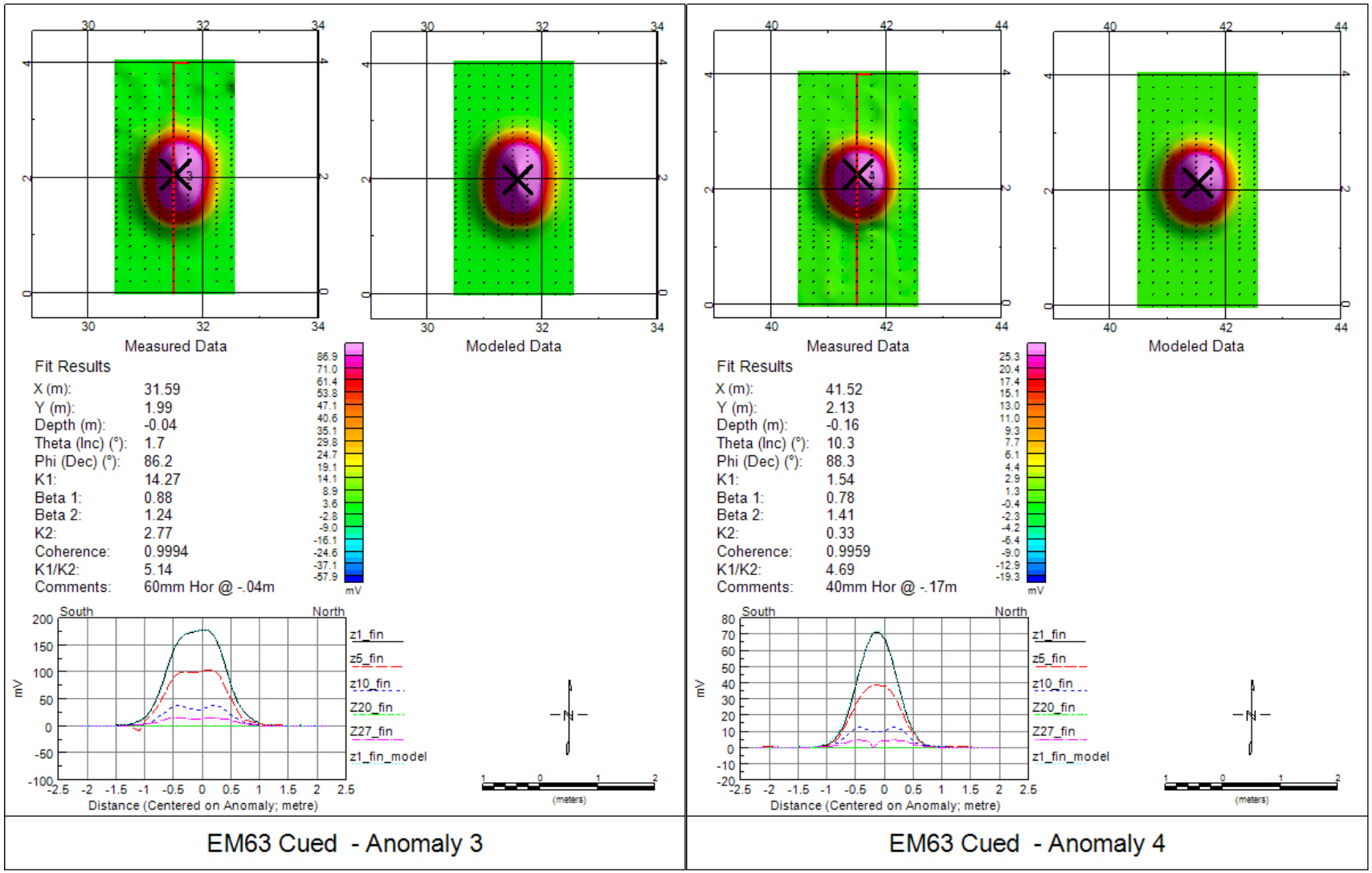

Figure 3-20 Anomaly plots of EM63 inversion results for 60mm (left) and 40mm (right) in a horizontal orientation.

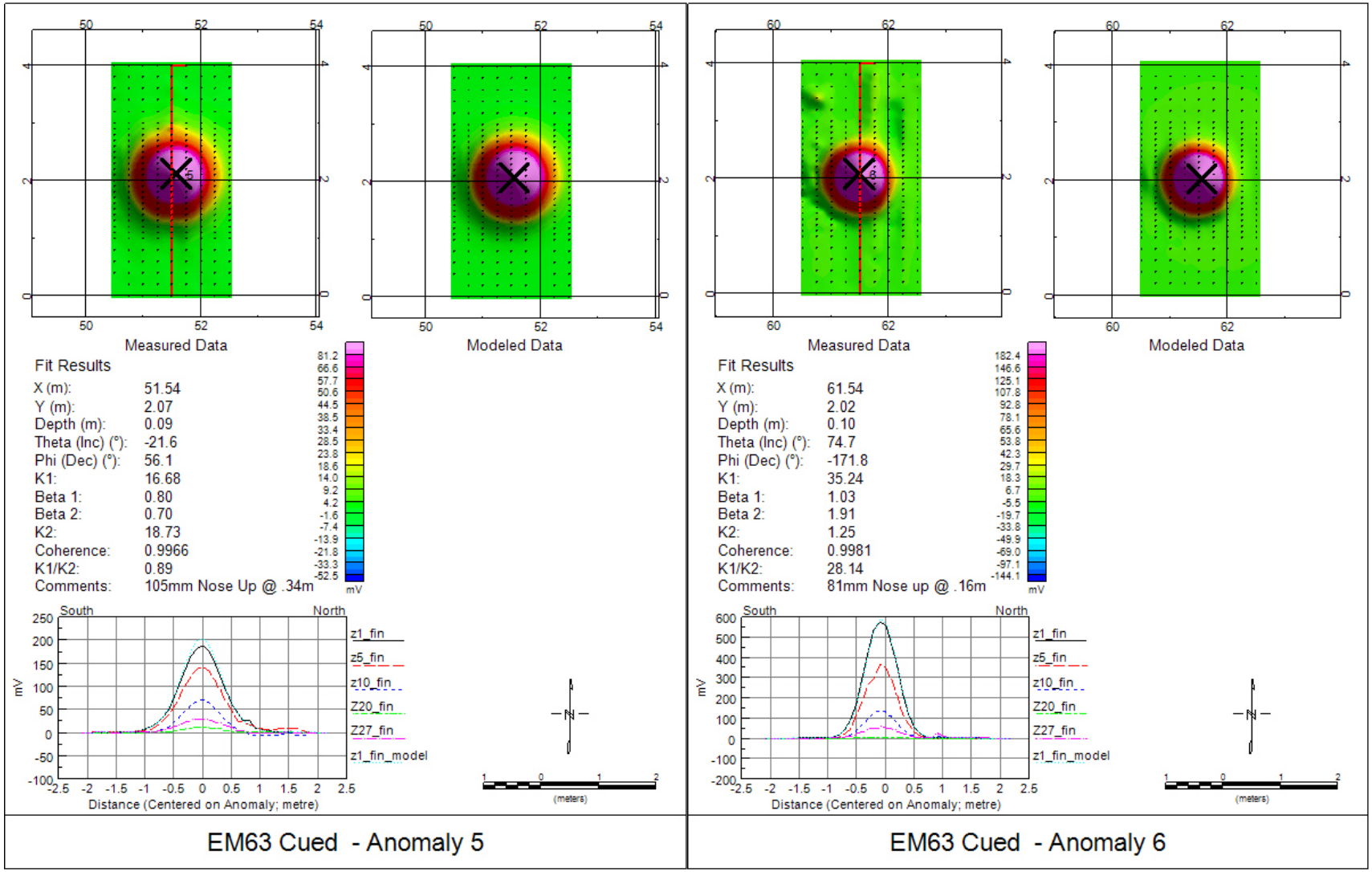

Figure 3-21 Anomaly plots of EM63 inversion results for 105mm (left) and 81mm (right) in a vertical nose up orientation.

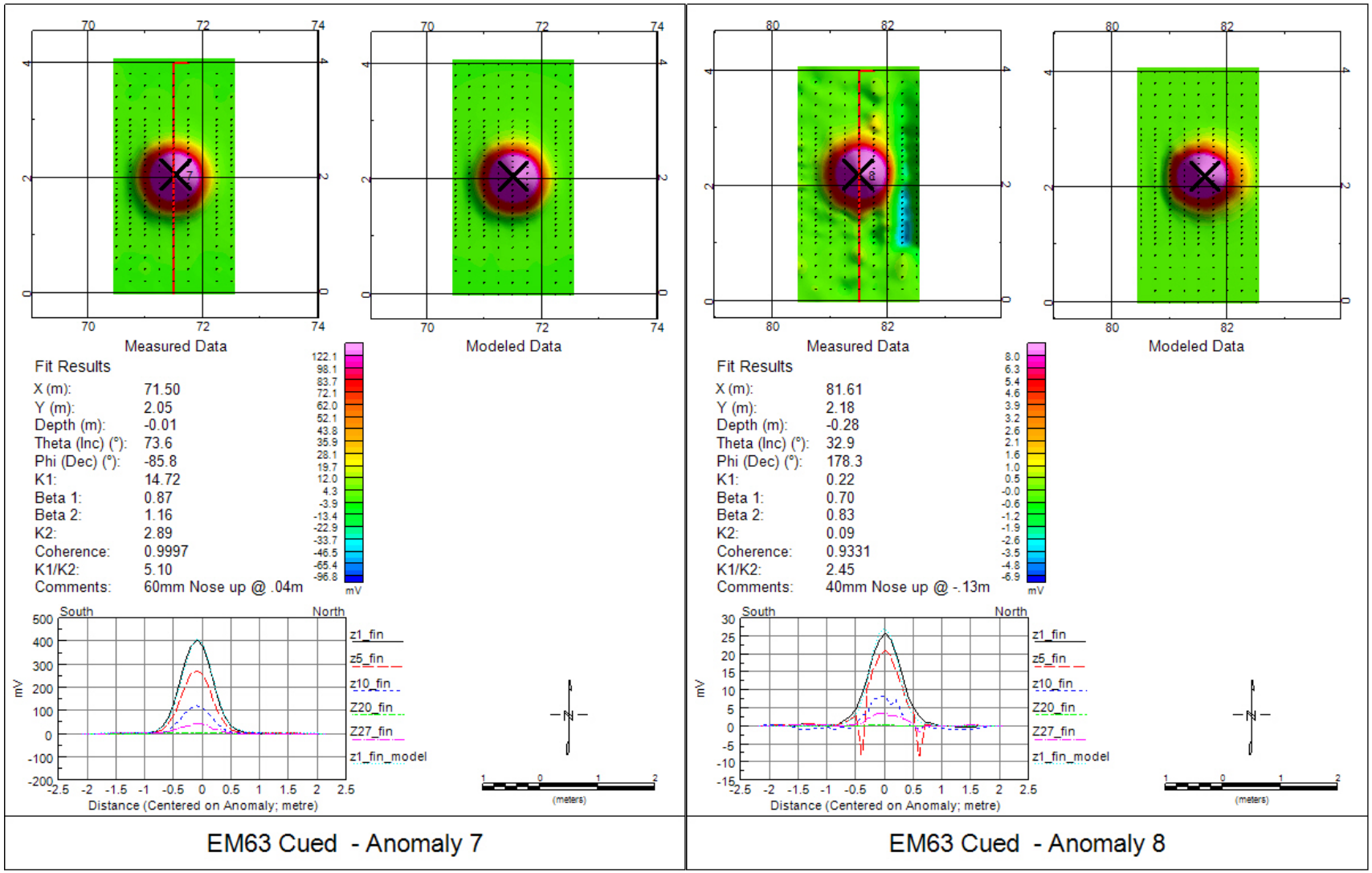

Figure 3-22 Anomaly plots of EM63 inversion results for 60mm (left) and 40mm (right) in a vertical nose up orientation. The data for some time gates were noisy (best illustrated in the profile section) resulting in the poor fit coherence for the 40mm.

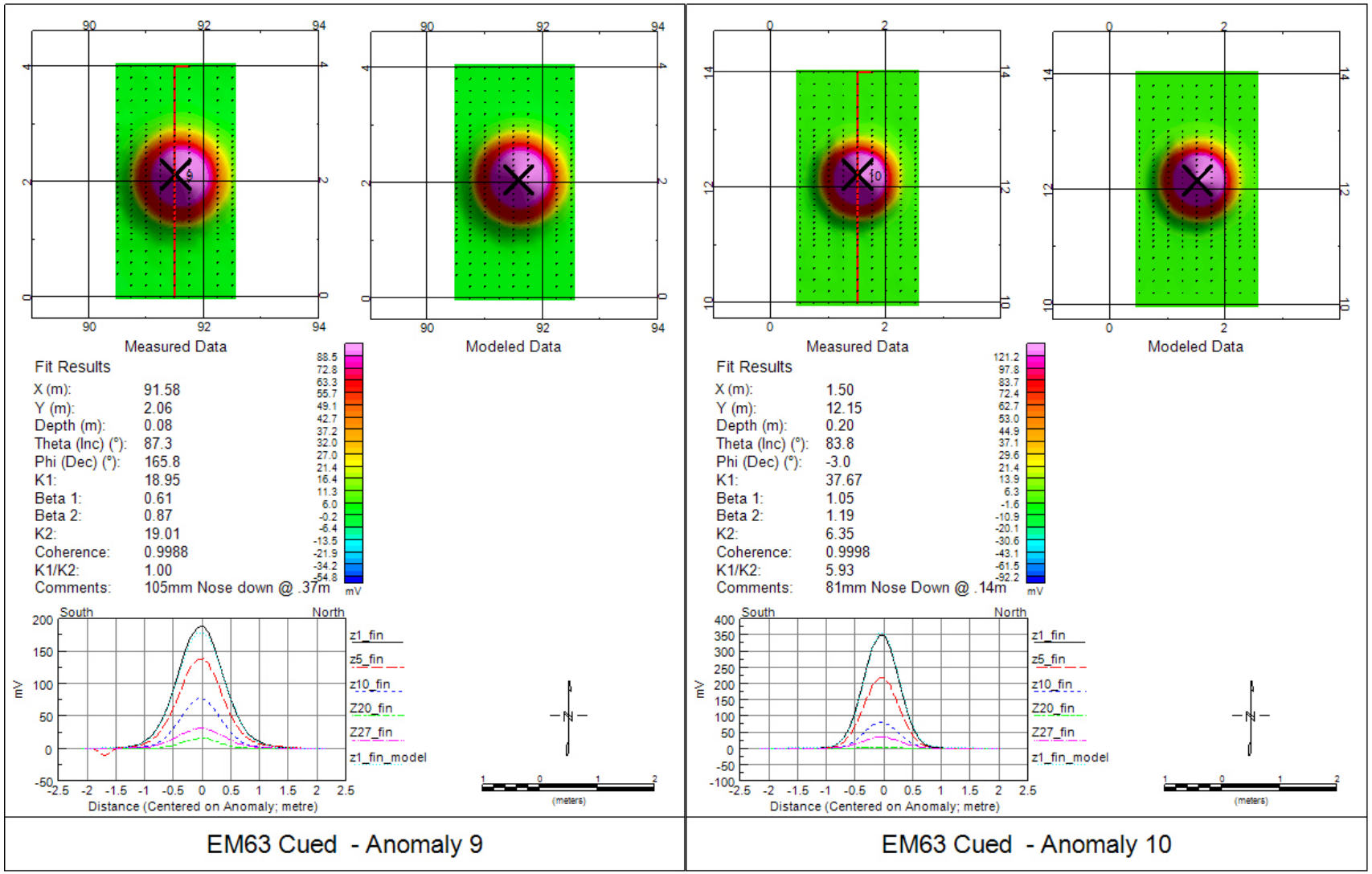

Figure 3-23 Anomaly plots of EM63 inversion results for 105mm (left) and 81mm (right) in a vertical nose down orientation.

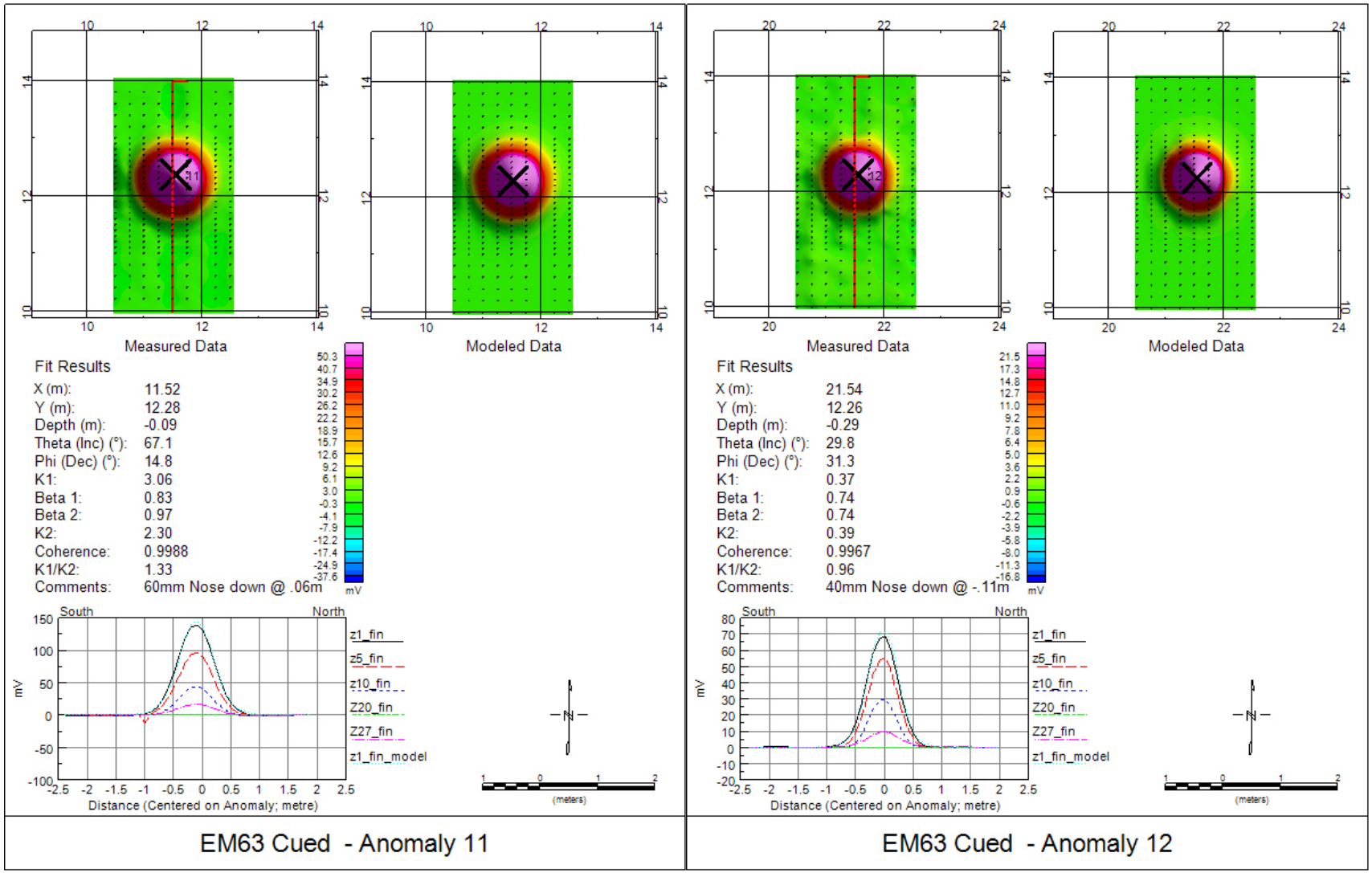

Figure 3-24 Anomaly plots of EM63 inversion results for 60mm (left) and 40mm (right) in a vertical nose down orientation.

4. Points of Contact

ESTCP

Anne Andrews	Program Manager, MM	Tel: 703-696-3826 Fax: 703-696-2114 anne.andrews@osd.mil
Katherine Kaye	Program Assistant, MM	Tel: 410-884-4447 Fax: 703-478-0526 kkaye@hgl.com

SAIC

Dean Keiswetter	Project Lead - SAIC	Tel: 919-677-1560 keiswetterd@saic.com
Tom Bell	Co-Project Lead	Tel: 703-414-3904 Thomas.H.Bell@saic.com
Tom Furuya	Data Analyst	Tel: 919-677-1563 furuyat@saic.com

Duke University

Leslie Collins	Project Lead - Duke	Tel: (919) 660-5260 Fax: (919) 660-5293 lcollins@ee.duke.edu

Geosoft Incorporated

Elizabeth Barayni	Oasis montaj Program Lead	Tel: (416) 369-0111 x356 Fax: (416) 369-9599 elizabeth.baranyi@geosoft.com